Climate Change in Taiwan

National Scientific Report 2024

Co-Published by National Science and Technology Council
and Ministry of Environment, R.O.C. (Taiwan)

Climate Change in Taiwan

National Scientific Report 2024

Edited by

Huang-Hsiung Hsu

Research Center for Environmental Changes
Academia Sinica

Ming-Hsu Li

Graduate Institute of Hydrological and Oceanic Sciences
National Central University

ISBN: 978-986-5436-59-9

Co-published : National Science and Technology Council (NSTC) & Ministry of Environment (MOENV) of Taiwan
Cover Photo: Mt. Jade South Peak, Taiwan
Photo by Chi, Po-lin, Provided by Chi Po-lin Foundation, © Above Taiwan Cinema, Inc.

Referencing this report:
NSTC & MOENV (2024). Climate change in Taiwan: National scientific report 2024 (H. H. Hsu & M. H. Li, Eds.). Co-published by National Science and Technology Council & Ministry of Environment, R.O.C. (Taiwan)

This edition first published Nov 2024

Authors

Chapter 1

Huang-Hsiung Hsu, Chia-Chi Wang, Shih-Yu Lee, Chun Hoe Chow, Yu-Chiao Liang
Yi-Chun Kuo, Chao-An Chen, Ying-Ting Chen, Yu-Heng Tseng, Wan-Ling Tseng
Jo-Hsu Huang, I-Chun Tsai, Chao-Chen Lai, Shih-How Lo

Chapter 2

Chia-Chi Wang, Jun Chiang, Ting-Hsuan Lee, Ching-Teng Li, Chi-Cherng Hong
Jien-Yi Tu, Huang-Hsiung Hsu, Yi-Chun Kuo, Ying-Ting Chen, Yu-Heng Tseng
Yu-Shiang Tung, Wan-Ru Huang, I-Chun Tsai, Tzu-Ting Lo

Chapter 3

Cheng-Ta Chen, Chun-Yu Wang, Chia-Chi Wang, Chia-Ying Tu, Szu-Ying Lin
Shiou-Li Lin, Huang-Hsiung Hsu, Yi-Chun Kuo, Chao-An Chen, Ying-Ting Chen
Yu-Heng Tseng, Yu-Shiang Tung, Wan-Ru Huang, I-Chun Tsai, Chao-Tzuen Cheng

Chapter 4

Ming-Hsu Li, Pao-Shan Yu, Dong-Sin Shih, Tao-Chang Yang, Hung-Wei Tseng
Tzu-Ming Liu, Yi-Hua Hsiao, Chi-Heng Lin, Ming-Lang Lin, Chi-Wen Chen
Fang-Yi Chu, Wei-Bo Chen, Chih-Hsin Chang, Ting-Yu Liang, Ming-Hwi Yao
Yung-Heng Hsu, Yu-Chen Liu, Yih-Min Shy, Di-Wang Chueh, Po-An Tu
Ching-Hsien Ho, Chih-Heng Cai, Bo-Yi Lu, Chia-Hsiang Chen, Ke-Yang Chang
Huan-Yu Lin, Yu-Yun Chen, Yu-Kai Chen, Ming-An Lee, Pau-Chung Chen
Shu-Li Julie Wang, Wei-Te Wu, Ching-Chun Lin, Tsung-Lin Tsai, Ruei-Syuan Wu
Shih-Liang Chan, Chia-Fa Chi, Tzu-Ping Lin, Si-Yu Yu, Liu-Chen Wang

Chapter 5

Shih-Liang Chan, Ming-Hsu Li, Yung-Ming Chen, Hsin-Chi Li, Chia-Fa Chi
Joyce Chang

Preface

This summary report provides an English version of the key contents of "Climate Change in Taiwan: National Scientific Report 2024" (hereinafter the Report), as required by Taiwan's "Climate Change Response Act," that was passed in early 2023. The Report is jointly issued by the National Science and Technology Council (NSTC) and the Ministry of Environment (MOENV).

The NSTC has long promoted climate change research and disseminated scientific findings to inform the public. The NSTC previously published a "Taiwan Climate Change Science Report" in 2011 and 2017. This Report continues the NSTC's mission to provide updates on scientific understanding in Taiwan climate change. The "Taiwan Climate Change Projection Information and Adaptation Knowledge Platform (TCCIP)" project began preparing this Report at the behest of the NSTC in the third quarter of 2022. After more than a year of effort, the editorial team completed the full Report, which contains more than 600 pages and more than 310,000 words authored by 68 individuals and reviewed by 25 experts.

Per the requirements of the Climate Change Response Act, the NSTC and the Ministry of Environment jointly held an interministerial meeting in March 2024 to solicit opinions on the Report drafted by the TCCIP project. After incorporating the changes suggested by the various ministries, the editorial team finalized the report and renamed it the "National Climate Change Science Report 2024: Phenomena, Impacts, and Adaptation."

Following the framework of previous NSTC climate change reports, this Report focuses on climate change science, impacts, and adaptation and is divided into five chapters. The first three chapters address climate change trends and projections, and the last two chapters cover impacts and adaptation. Chapter 1 examines climate change globally and in East Asia in particular. Chapters 2 and 3 analyze Taiwan's climate trends and projections. Chapter 4 compiles information on challenges such as the impacts of climate on water resources, slope land, coastal areas, food security, ecology, health, and urban–rural planning. Chapter 5 explores scientific discourse on climate risk and adaptation, offering a reference for ministries and local governments in their planning of adaptation strategies.

The Report consolidates crucial Taiwanese and international data on climate observations, projections, impact research, and adaptation methods, updating key findings on climate change from the 2017 Science Report. This Report cites more than 1,200 academic articles and ministry reports published before June 2023 and incorporates more than 600 review comments from experts, scholars, and ministries concerning accuracy, scientific discourse, citations, and interpretations.

Editor

Huang-Hsiung Hsu *Ming-Hsu Li*

Contents

Chapter 1

GLOBAL AND EAST ASIAN CLIMATE CHANGE

1. Global warming has accelerated considerably since 1850. Between 2001 and 2020, global surface air temperatures were 0.99°C (0.84°C to 1.10°C) higher than the 1850–1900 baseline. Temperatures have increased sharply since 2012, with 2016–2020 recorded as the hottest 5-year period since 1850. Warming has been uneven, with land areas warming more than oceans, and polar regions warming more than regions at mid- and low-latitudes, particularly those in the Northern Hemisphere.

2. Climate attribution studies have demonstrated that anthropogenic greenhouse gas emissions were the primary driver of late-20th-century warming, with natural forces playing a minor role.

3. Projections under various Shared Socioeconomic Pathways (SSPs) indicate that global mean surface air temperatures will increase until at least the mid-21st century. By the century's end, temperatures are projected to have risen by between 1.0°C and 1.8°C under the low-emission scenario (SSP1-1.9) and between 3.3°C and 5.7°C under the high-emission scenario (SSP5-8.5). Warming beyond 2°C is likely to occur between 2041 and 2060 under SSP5-8.5. Other scenarios suggest that warming beyond 1.5°C will occur in the early 2030s. All projections indicate that the Northern Hemisphere will warm to a greater degree than will the Southern Hemisphere, with land warming more than the oceans and the highest warming rates occurring at high latitudes.

4. Since the 1950s, the intensity and frequency of extreme heat events have increased in most regions of the globe, whereas the intensity and frequency of extreme cold events have decreased. The increase in greenhouse gas emissions due to human activities is the primary driver of these changes. Extreme heat events and heatwaves are projected to become more frequent and intense in most regions, particularly over land areas.

5. Observational records since 1950 reveal a slight increasing trend in global land precipitation, although regional patterns vary. Between 1980 and 2019, precipitation increased in tropical regions, tropical Africa, parts of Europe and Central Asia, and the Maritime Continent but decreased over central South America, western North America, northern Africa, and the Middle East.

6. Global mean precipitation will increase as greenhouse gas concentrations increase, and will be greater over land than over the oceans. Specifically, for each 1°C of global warming, mean precipitation may increase by between 2% and 3%. Short-term (2021–2040) precipitation projections exhibit greater uncertainty than do those for the end of the century, for which the differences in precipitation between scenarios are less pronounced. Uncertainty is due to natural climate variability, climate models, and the effects of aerosols. The Northern Hemisphere temperate zone will experience a faster precipitation increase than the global land average.

7. Comprehensive land observations since the 1950s reveal increasing trends in the frequency, intensity, and amount of heavy precipitation events that are primarily attributable to human factors. These trends indicate that, for each 1°C of warming, the frequency and intensity of extreme precipitation will increase by approximately 7%. Projections also indicate that the frequency of extreme precipitation will likely increase in nearly all land areas as global warming intensifies, with now-rare extreme events increasing at higher rates.

8. Limited evidence is available regarding trends in meteorological drought, and regional trend estimates are inconsistent and highly uncertain. As global warming intensifies, the frequency, intensity, and likelihood of regional droughts are projected to increase; meteorological droughts are expected to become more frequent and severe and to affect larger areas.

9. Observational records reveal an increasing trend in the proportion of global tropical cyclones of categories 3–5 and the frequency of rapid intensification events. Tropical cyclone activity in the Western North Pacific is shifting poleward. Additionally, projections indicate that the rainfall and intensity of tropical cyclones as well as the proportion of intense tropical cyclones will increase with warming. By the end of the 21st century, the number of typhoons in the Western North Pacific is expected to have decreased; those that occur will have a shorter lifespan and exhibit a poleward shift, although maximum wind speeds and rainfall will increase.

10. Compound events—those combining multiple extreme hazards—are likely to become more frequent or severe in a warming future in most regions.

11. Historical data reveal a rising trend in sea surface temperatures (SST) across most ocean basins, with the greatest warming occurring in the high latitudes of the Northern Hemisphere. Since 1850, global average SST have increased by 0.88°C, with 0.60°C of this increase occurring after 1980. Climate models project SST increases of 0.86°C under SSP1-2.6 and of 2.89°C under SSP5-8.5 by the end of this century. Rising SST will also likely increase the frequency of marine heatwaves and ocean stratification.

12. Observations indicate that the global ocean pH has been gradually declining since 1950 in a clear trend toward acidification. Projections under all emission scenarios indicate that this acidification trend will become more pronounced with increased warming. Warming-induced acidification will adversely affect the ocean's ability to absorb carbon dioxide, weakening its carbon sink function.

13. Observational evidence is inconclusive regarding whether the Atlantic Meridional Overturning Circulation (AMOC) is weakening and whether this trend is due to natural variability or human influence. However, projections under warming scenarios indicate a clear weakening trend in the AMOC. Hydrographic data suggest that the Kuroshio Current has generally accelerated and shifted offshore in the period 1955–2010, with this trend being more pronounced in summer.

14. Sea ice observations reveal substantial declines in Arctic sea ice, especially during the formation stage in September. Although Antarctic sea ice is exhibiting less of a decline, the data indicate a rapid decrease in recent years. All warming scenarios project substantial decreases in Arctic and Antarctic sea ice. Under the highest-emission scenario (SSP5-8.5), Arctic sea ice in September may disappear entirely by 2050. By contrast, under low-emission scenarios (SSP1-2.6 and SSP1-1.9), Arctic sea ice is not projected to disappear by the century's end.

15. Observations indicate that the rate of mass loss of two major global ice sheets, Greenland and Antarctica, is increasing and that this is contributing to a global sea level rise. Long-term observations of glacier mass and Northern Hemisphere spring snow cover also reveal decreasing trends. However, snow cover has increased in some regions such as North America and Siberia. Additionally, observations indicate an increase in permafrost temperatures.

16. Projections under all emission scenarios indicate that both the Greenland and Antarctic ice sheets will continue to decrease in size throughout this century. Glacier volume, the volume of ground permafrost, and the Northern Hemisphere seasonal snow cover will almost certainly decline.

17. Sea levels have fluctuated over the past 800,000 years, but the global mean sea level has risen at an increasing rate since the mid-19th century, surpassing the average rate of the previous two millennia. The 20th century's sea level rise was the highest in the past three millennia, with a marked acceleration in the last two decades. Human-induced warming, causing thermal seawater expansion, has been the primary driver. Under warming scenarios, sea levels will continue to rise at an accelerated pace. By the end of the 21st century, sea levels are projected to have increased by between 0.38 meters (SSP1-1.9) and 0.77 meters (SSP5-8.5). Thermal expansion will remain the dominant factor driving this change. After 2100, deep ocean heat absorption and ice sheet melt will continue to raise sea levels.

18. Observations reveal multidecadal variabilities in Northern Hemisphere monsoon circulation and rainfall since 1900. Since 1980, the Northern Hemisphere monsoon has exhibited higher rainfall and a longer summer season. The Southern Hemisphere monsoon is influenced by strong interannual variability and regional differences, and no significant long-term trends are discernable in the observational data. Overall, no notable trend is discernable in global monsoons because of the influence of substantial interannual and decadal variations and regional differences.

19. Projections suggest that global monsoon rainfall may increase, whereas monsoon circulation may weaken, primarily due to an increase in moisture. Spatially, the increase in monsoon rainfall exhibits marked north–south asymmetry, with a larger increase in the Northern Hemisphere than in the Southern Hemisphere. Monsoons in Asia and Africa will strengthen, whereas those in North America will weaken.

20. Anthropogenic aerosol emissions have an adverse effect on monsoon rainfall in South Asia and East Asia. However, projections indicate increasing monsoon rainfall in all regions, primarily due to the increase in greenhouse gases.

21. East Asia is projected to experience increased monsoon rainfall due to earlier-onset and longer summers, mainly contributed by the strengthening of the Meiyu rain band. The increase will be most pronounced in Southeast Asia and southern China. Monsoon rainfall will increase in all scenarios, becoming more pronounced by the century's end as greenhouse gas concentrations rise. However, model projections of monsoon rainfall remain uncertain due to factors such as aerosol emissions, human influence, and internal climate variability. Nevertheless, increased rainfall can be projected with high confidence, and longer monsoon seasons can be projected with medium confidence.

22. Projections under the high-emissions scenario (RCP8.5) indicate a poleward shift in regions of higher frequency of frontal systems. Winter projections (2071–2100) indicate a slight decrease in frequency of frontal systems in the polar front region and subtropics, with a slight increase between the Yellow and Yangtze Rivers, on the Korean Peninsula, in Japan, and in the Pacific east of Japan. Additionally, a substantial rise in frontal activity is expected south of 20°N over the Philippine Sea and east of Taiwan. In spring, frequency of frontal systems will considerably increase between 30°N and 40°N, particularly along the coast north of the Yangtze River and in Japan, but will decrease between 20°N and 30°N, especially from South China to Taiwan.

23. From 1850 to the 1970s, concentrations of aerosols and their precursors increased, leading to a cooling effect that partially offset greenhouse-gas-induced warming. Since the mid-1970s, efforts to reduce aerosol emissions have improved air quality, weakening the net radiative cooling effect. Between 2010 and 2019, global carbon monoxide levels declined, and sulfur dioxide and nitrogen dioxide decreased in North America and Europe but increased in South Asia and rose before falling in East Asia. Ozone concentrations have increased globally except in the western United States and Europe.

24. Global warming accelerates ozone depletion, leading to a decrease in surface ozone in low-pollution areas but exacerbating pollution. Under the high-emission scenario (RCP8.5), global warming is projected to increase average aerosol concentrations by approximately 0.21 mg m^{-3} by 2100. Therefore, the increased frequency of heatwaves will increase the concentrations of high-pollution ozone and aerosols. Global warming causes changes in large-scale circulation, including an increase in the Arctic Oscillation Index and a weakening of the winter monsoon, rendering Asia prone to high-pollution events in winter.

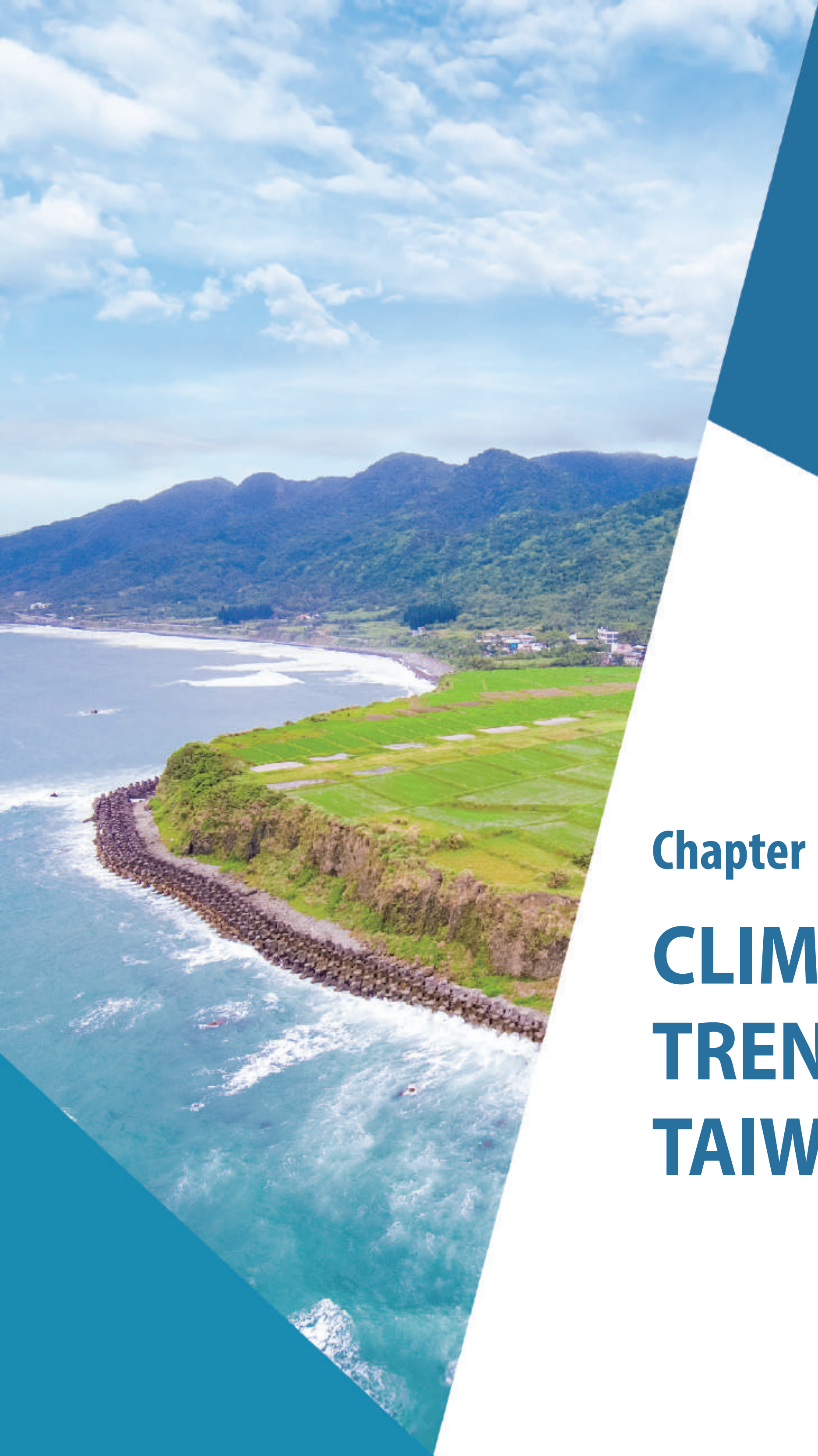

Chapter 2 CLIMATE CHANGE TRENDS IN TAIWAN

1. Long-term temperature trends at various weather stations across Taiwan reveal consistent warming along with low-frequency oscillations. The warming trend has intensified as time progresses toward the present. Stations with more than a century of data reveal that the average warming rate has risen from 0.15°C to 0.27°C per decade. During the summer half of the year (May to October), the rate has increased from 0.15°C to 0.32°C, and in the winter half-year (November to April), it has risen from 0.15°C to 0.29°C since the mid-1970s. However, the winter warming trend has slowed since the 1990s (statistically insignificant).

2. Observations from six weather stations with more than a century of data (Taipei, Taichung, Tainan, Hengchun, Hualien, and Taitung) provided by the Central Weather Administration (CWA) reveal that the average air temperature gradually increased from 1920 to 1940, remained stable from 1940 to 1980, and rose considerably after 1980. The temperature increase after 1980 was notably greater than that in other periods. The warming rates since the 1990s, since the 1970s, and in the long term (1900 to 2022) are 0.27°C, 0.25°C, and 0.15°C per decade, respectively (Figure 2-1).

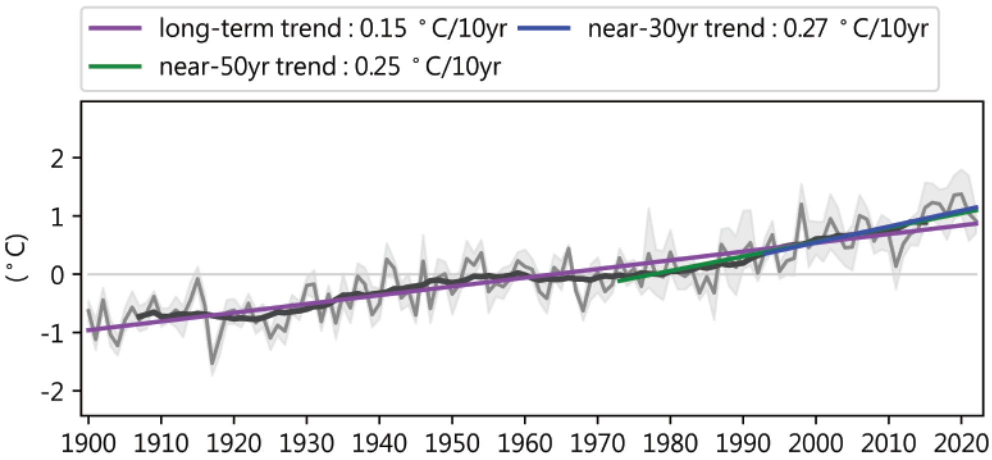

Figure 2-1
Trends and annual average surface air temperature anomaly in Taiwan from 1900 to 2022 (six CWA stations with observations exceeding 100 years)

3. The warming trends in temperature observed in data from stations in Taiwan are more pronounced in the winter half-year than in the summer half-year. The increase in the daily minimum temperature is also more pronounced than the increase in the daily maximum temperature, which is primarily responsible for the narrowing of the diurnal temperature range.

4. Over the past century, the beginning of summer has moved earlier, and the end of summer has moved later, resulting in a longer summer season. The highest temperatures have consistently increased. Conversely, the beginning of winter has moved later, and the end of winter has moved earlier, leading to a shorter winter season. The lowest temperatures have also consistently increased. Additionally, the timing of peak maximum and minimum temperatures shows little variation. Overall, summer has lengthened by between 6.31 and 12.88 days per decade, whereas winter has shortened by between 6.19 and 12.20 days per decade since the 1970s（Figure 2-2）.

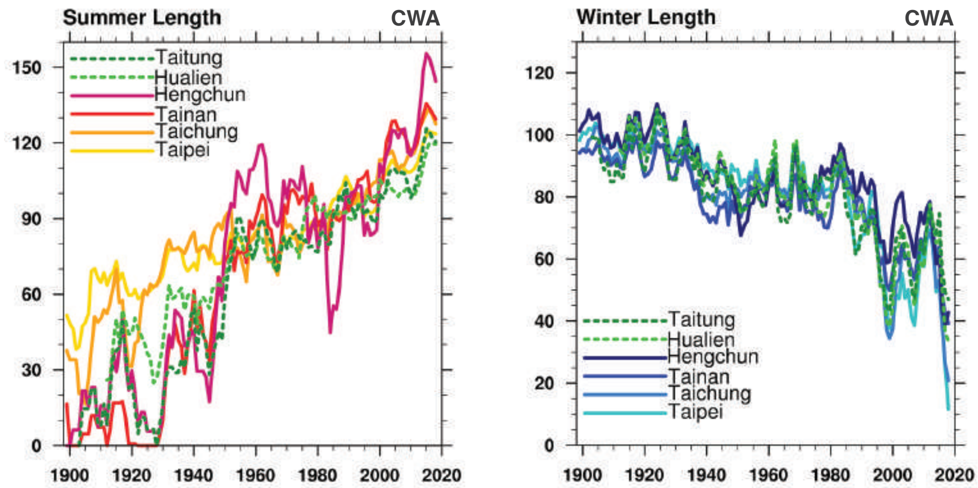

Figure 2-2
The lengths of summer (left) and winter (right) in six CWA stations in Taiwan.

5. Observational records from Taiwan reveal nonsignificant long-term trends in annual precipitation and seasonal precipitation, which are influenced by interannual and interdecadal oscillations (Figure 2-3).

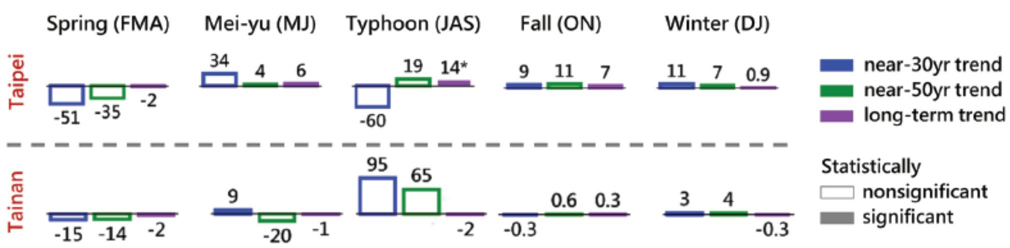

Figure 2-3
Seasonal precipitation trends in Taipei (upper) and Tainan (lower) stations in spring, mei-yu, typhoon, fall and winter (from left to right). The unit is mm/decade. The asterisk represents that values are statistically significant at the 5% level.

6. Wind station-based observations in Taiwan indicate a decline in the annual mean wind speed, maximum wind speed, and seasonal mean maximum wind speed, although these trends are also influenced by interdecadal low-frequency oscillations.

7. The regional SST and sea level changes associated with global warming pose critical challenges for marine ecosystems and marine and coastal industries. For example, observational data for the Taiwan Strait indicate a long-term trend of increasing SSTs over the past century. After the decadal stalling of SST increase during the global warming hiatus from 1998 to 2012, SST has resumed the warming trend. From 2012 to 2018, the warming trend was approximately 0.63°C per decade, and this rate is projected to continue to increase until the end of this century (Yamanaka et al., 2021) (Figure 2-4). Tide gauge and satellite data demonstrate that annual mean SSTs in the Taiwan Strait have increased 0.23°C per decade from 1957 to 2016. The trend in sea level rise (2.2 ± 0.3 mm per year from 1993 to 2015) was slightly smaller than that in the global average (3.2 ± 0.1 mm per year from 1993 to 2012).

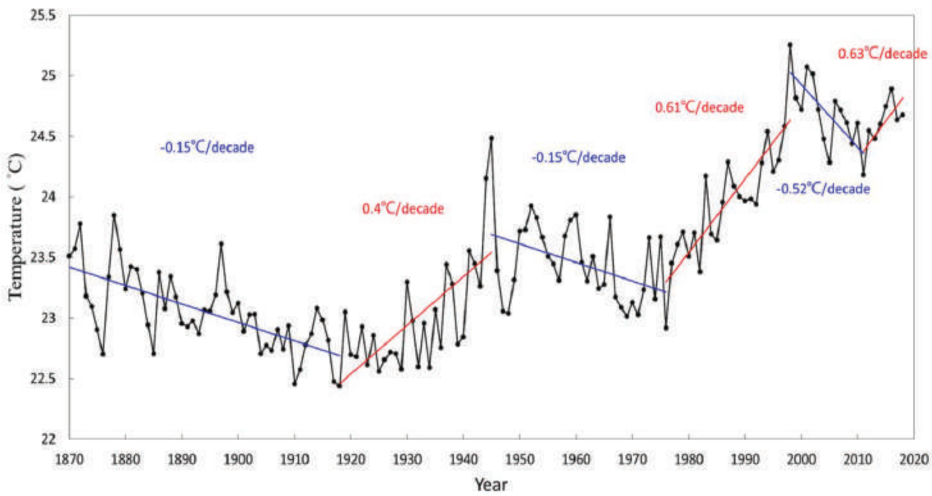

Figure 2-4

Time series of annual mean sea surface temperatures in the Taiwan Strait from 1870 to 2020 (Lee et al., 2021)

8. Station-based observational data indicate that the number of days with extremely high temperature has increased, whereas the number of days with extremely low temperature has decreased (Figure 2-5).

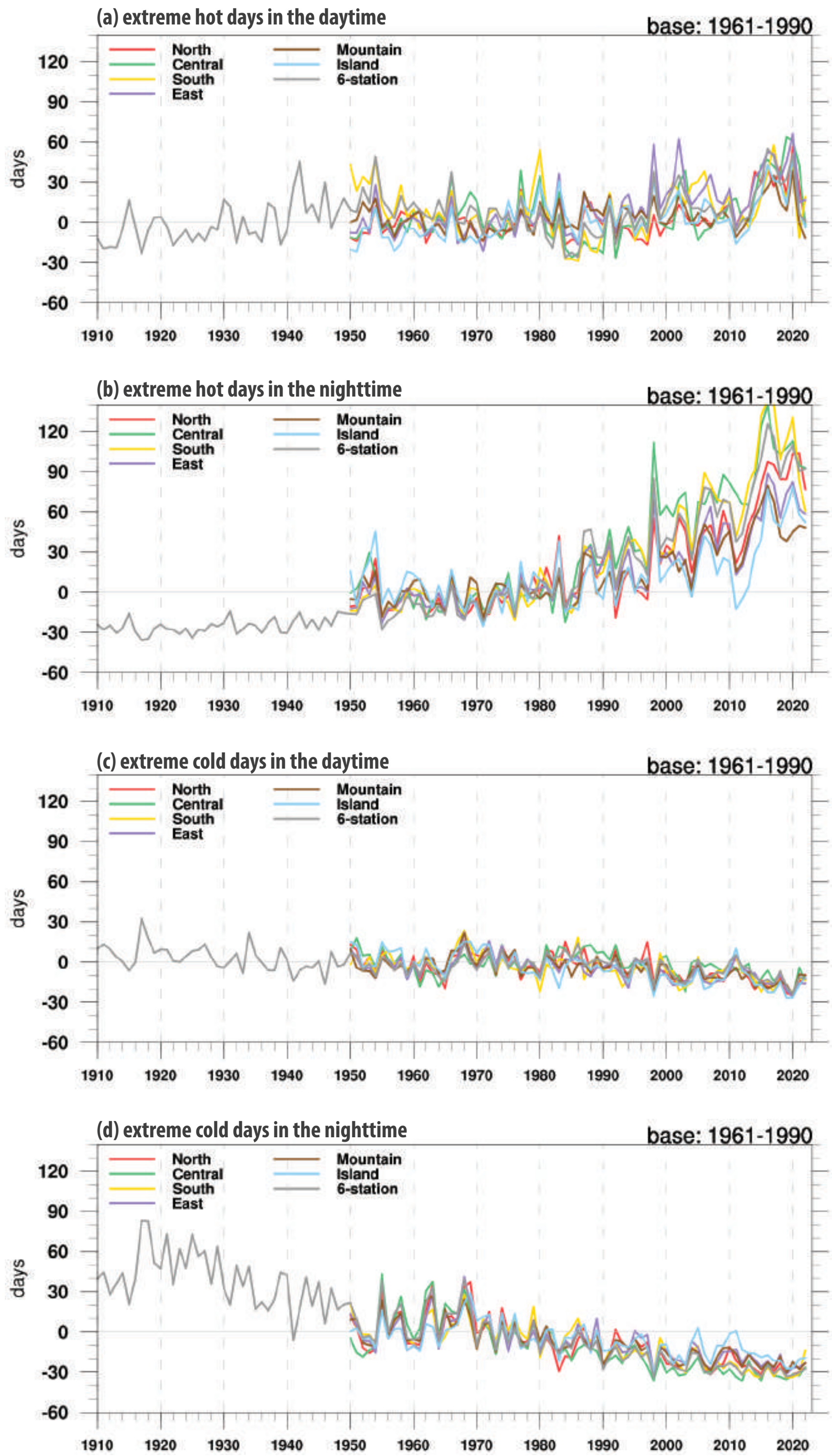

Figure 2-5

The historical changes of extreme hot and cold days. The number of (a) extreme hot days in the daytime (TX90p); (b) extreme hot days in the nighttime (TN90p); (c) extreme cold days in the daytime (TX10p); (d) extreme cold days in the nighttime (TN10p). Color curves indicate average in the northern Taiwan (red), central Taiwan (green), southern Taiwan (yellow), eastern Taiwan (purple), mountain area (brown), outer islands (blue), and 6 century-long stations (grey).

9. Changes in the number of days with extreme daily rainfall (80 mm, 200 mm, and 350 mm) do not exhibit a consistent pattern across regions in observational data, nor do they exhibit a significant long-term trend. However, the fluctuation of interannual variability in mountainous areas has increased since 2000 (Figure 2-6).

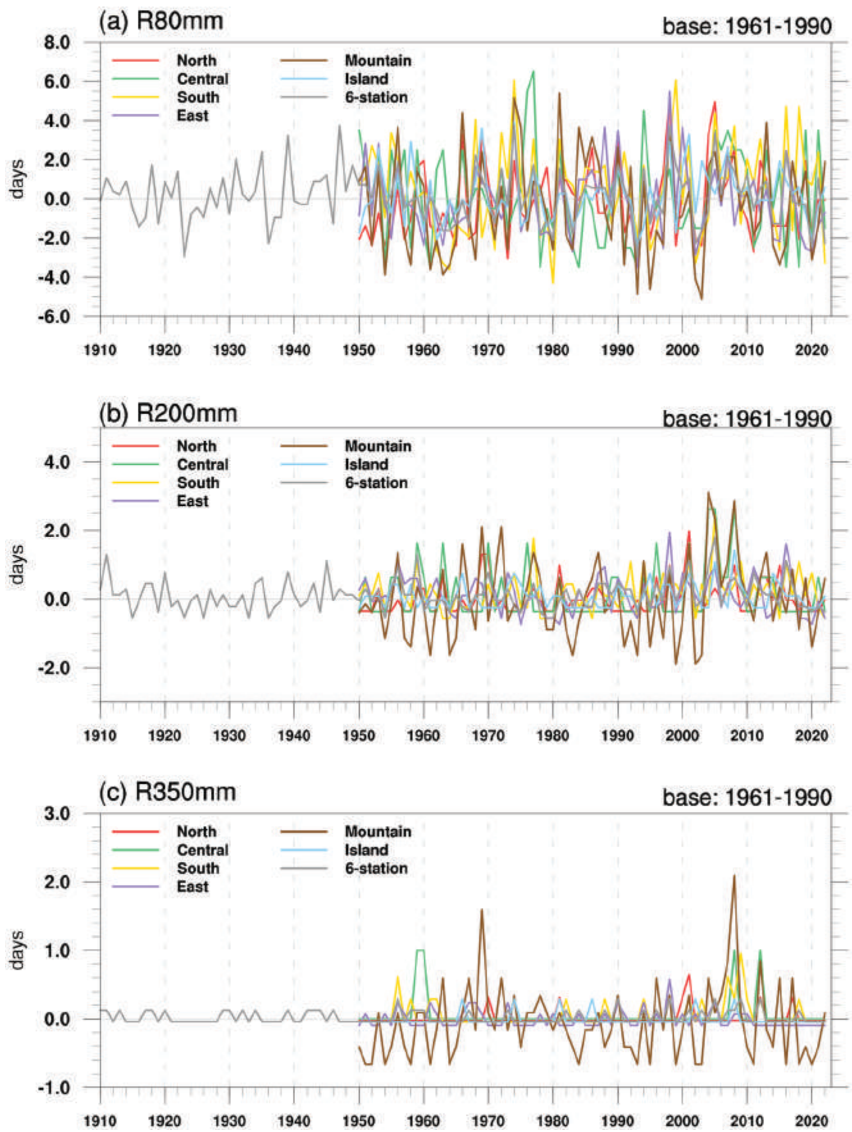

Figure 2-6

The historical changes in the number of days with precipitation rate greater than (a) 80 mm/day, (b) 200 mm/day and (c) 350 mm/day. Color curves indicate average in the northern Taiwan (red), central Taiwan (green), southern Taiwan (yellow), eastern Taiwan (purple), mountain area (brown), outer islands (blue), and 6 century-long stations (grey).

10. Analysis of a century-long station data indicates that the frequency of winter cold surges and the number of consecutive cold days have decreased significantly. For example, in Taipei, the annual frequency of cold surges has decreased by approximately 3.8 events and the annual number of cold days has decreased by approximately 14.5 days since the 1970s.

11. The maximum number of consecutive dry days (CDD) and the standardized precipitation index (SPI12) in observational station data do not exhibit long-term trends. However, fluctuations of interannual variability in the CDD and SPI12 have increased at central and southern stations. Meteorological droughts have occurred more frequently at the Tainan, Hengchun, and Taitung stations since 1960 (Figure 2-7).

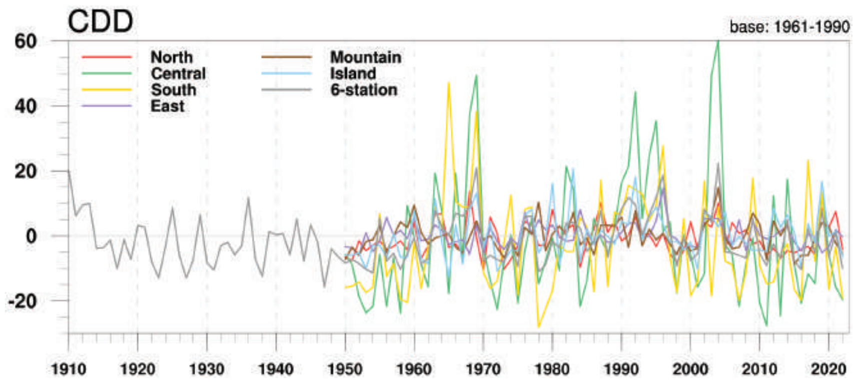

Figure 2-7

The maximum number of consecutive dry days (CDD) in CWA stations. Color curves indicate average in the northern Taiwan (red), central Taiwan (green), southern Taiwan (yellow), eastern Taiwan (purple), mountain area (brown), outer islands (blue), and 6 century-long stations (grey).

12. Meteorological droughts exhibit distinct regional differences in frequency and are influenced by low-frequency oscillations. Low rainfall is related to large-scale circulation conditions.

13. No long-term trends are discernible in the number of typhoons and intense typhoons affecting Taiwan. The number of typhoons exhibits characteristics of interdecadal variability (Figure 2-8).

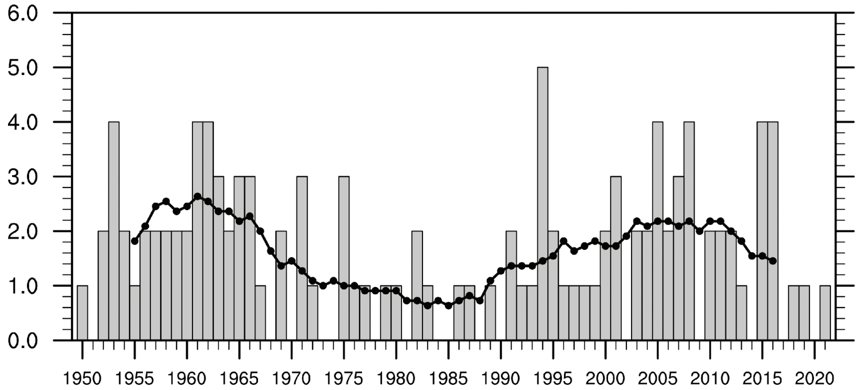

Figure 2-8

The annual number of intense typhoons affecting Taiwan from 1950 to 2021. Black curve indicates the 11-year running mean.

14. Changes in typhoon tracks are influenced by large-scale circulation and are not significantly correlated with global warming.

15. The frequency and intensity of afternoon convection in northern Taiwan during summer (June to August) has generally increased but has decreased in mountainous areas. By contrast, the frequency of convection in the central and southern plains has decreased, whereas the intensity has increased (Figure 2-9).

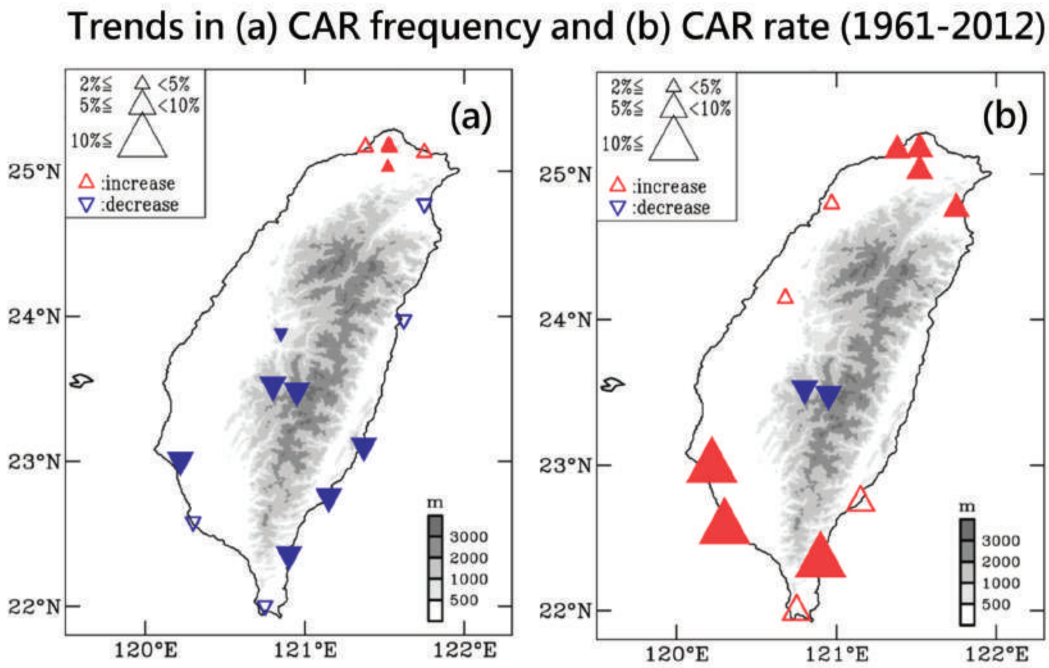

Figure 2-9

The historical trends of summer (JJA) Convective Afternoon Rainfall (CAR) (a) frequency and (b) intensity based on 1961-2012 CWA station data.

16. During the Meiyu season (May and June), the rainfall amount, rainfall intensity, and extreme rainfall intensity (PR90) for May have all exhibited increasing trends, but the trends have not been found for June.

17. The frequency and intensity of afternoon convection during the Meiyu season have increased.

18. Observational data reveal that the average concentrations of various pollutants that affect air quality in Taiwan have decreased since the 1990s. However, an increasing trend is found in the concentration of human-produced nitrate.

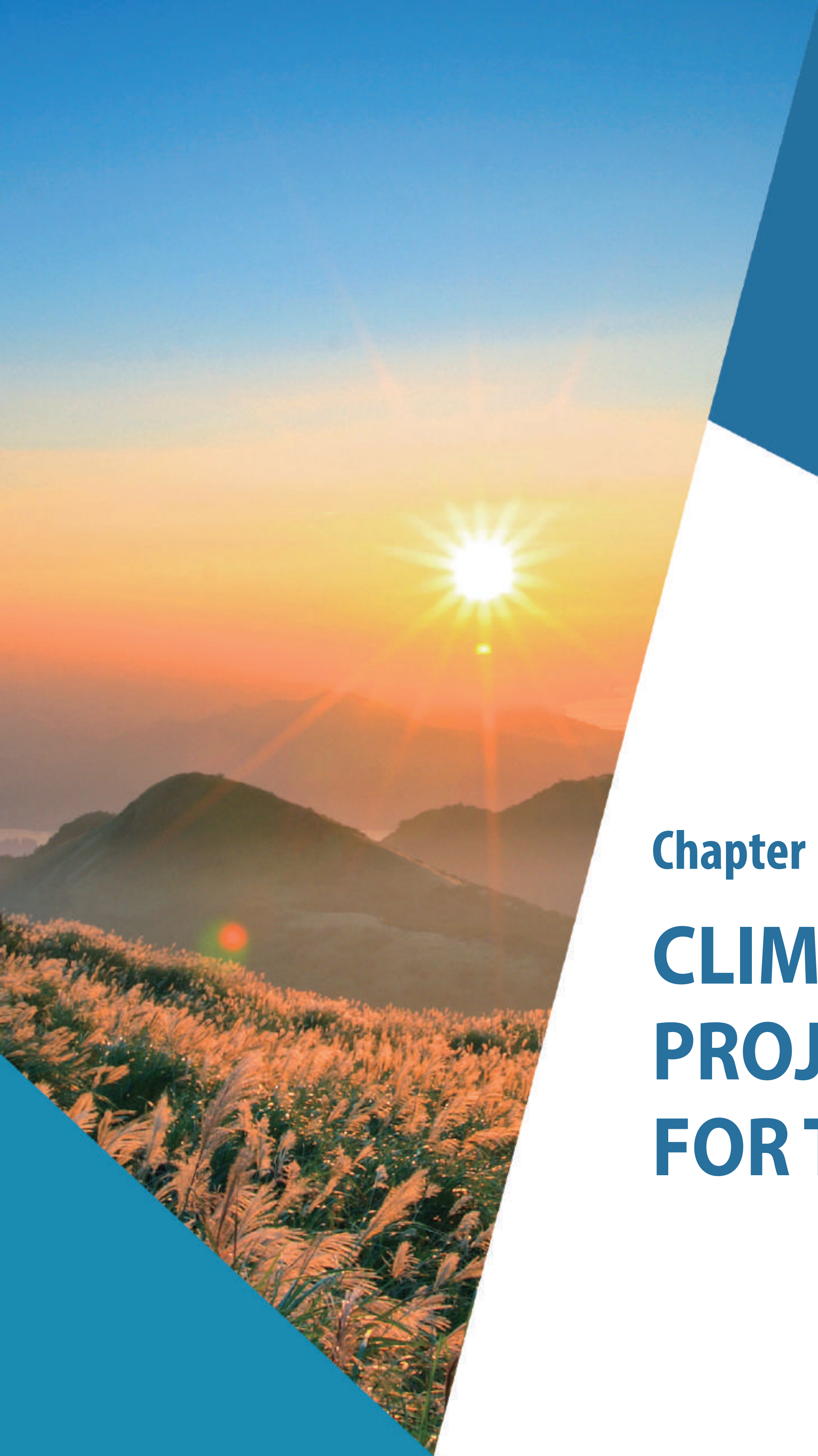

Chapter 3

CLIMATE CHANGE PROJECTIONS FOR TAIWAN

1. The future projection of Taiwan are obtained from statistical downscaling of Coupled Model Intercomparison Project Phase 6 (CMIP6) model data. Analyses compare three 20-year periods—the short term (2021–2040), mid-term (2041–2060), and long term (2081–2100)—relative to the baseline (1995–2014). Under the four SSP scenarios, the projections of average temperature in Taiwan increase by 0.6°C to 0.8°C in the short term. In the long term, warming will vary from 1°C under SSP1-2.6 to 3.4°C under SSP5-8.5. The most substantial warming is over northwestern Taiwan.

2. When comparing the three 20-year periods to Global Warming Levels (GWLs)—the rise in global average temperature relative to pre-industrial levels—GWL of 1.5°C corresponds to the short-term period, GWL of 2°C to the mid-term period, and GWL of 3°C and 4°C, to the long-term period, depending on the degree of mitigation. GWLs start to reach 1.5°C and 2°C in the 2030s and 2040s respectively. Therefore, GWL of 1.5°C may be referred to the short-term period, GWL of 2°C to the mid-term period, and GWL of 3°C and GWL of 4°C, to the long-term period (Figure 3-1).

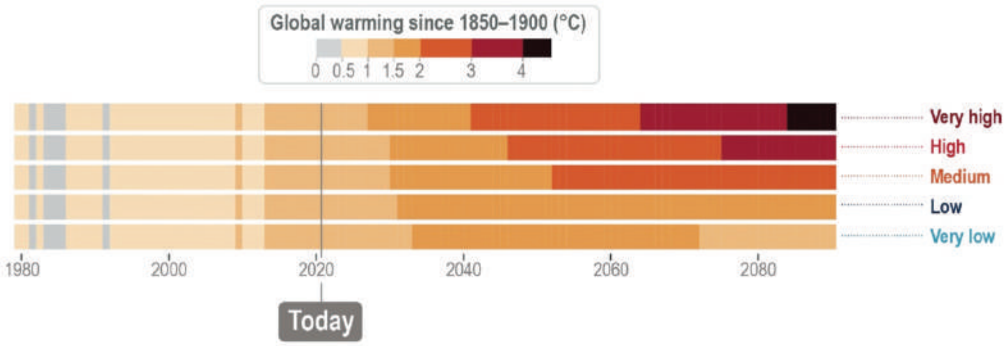

Figure 3-1

Projected warming for each of these emissions scenarios (very low: SSP1-1.9, low: SSP1-2.6, medium: SSP2-4.5, high: SSP3-7.0, very high: SSP5-8.5). (Adapted from the IPCC Assessment Report 6 [AR6], working group I [WGI], Infographic TS.1.)

3. Under various GWLs, the median temperature increases in Taiwan range from 0.6°C to 2.7°C for GWLs of 1.5°C to 4°C.

4. Global surface air temperatures have steadily risen over the past century, primarily due to increasing anthropogenic greenhouse gas emissions. On the basis of the CMIP6 climate projections under the four SSP scenarios, warming in Taiwan will continue at least until the middle of the century.

5. In the short term (2021 to 2040), the range of average air temperature increases across scenarios is nonsignificant, with a projected warming of 0.6°C to 0.8°C (median), relative to 1995-2014. In the mid-term (2041–2060), the difference between scenarios is greater: the low-emission scenario (SSP1-2.6) projects a temperature increase of 1°C, whereas the very high-emission scenario (SSP5-8.5) projects a temperature increase of 1.6°C. By the long term (2081–2100), the differences between scenarios are highly pronounced. Under the low-emission scenario, the warming could be maintained at the mid-term rate of approximately 1°C, but under the very high-emission scenario, the warming could increase by 3.4°C (Figure 3-2).

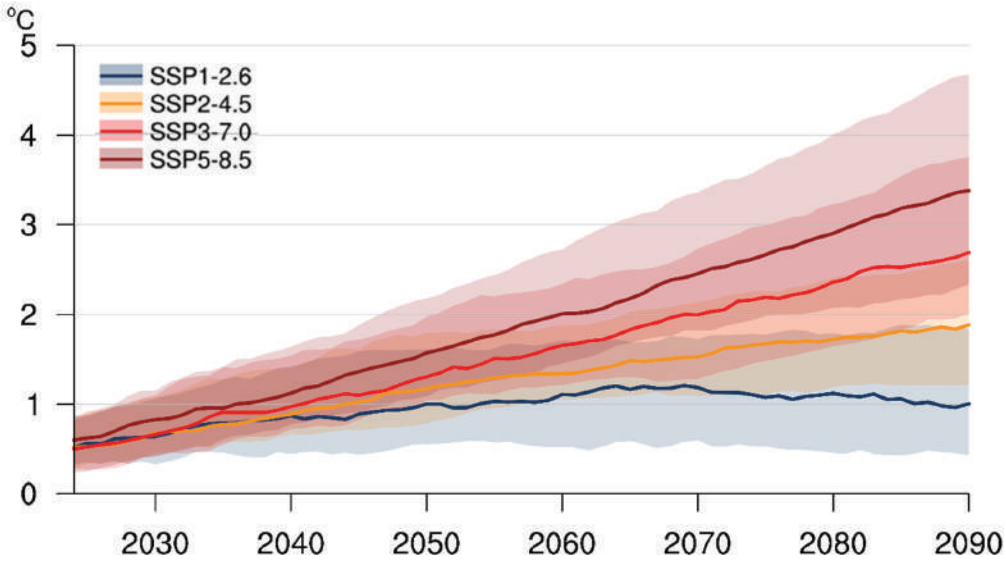

Figure 3-2

Projected change in 20-year running mean surface air temperature in Taiwan for four scenarios (central estimate solid, very likely range shaded), relative to 1995–2014.

6. Observations and projections indicate a consistent trend in the length of the seasons based on temperature (Figure 3-3): under the SSP5-8.5 scenario, summer will continue to lengthen and will exceed 210 days by the end of the century. By contrast, winter will continue to shorten to fewer than 30 days, potentially disappearing as early as the winter of 2060 in the very high-emission scenario. As such, Taiwan's temperature characteristics will more closely resemble those of other tropical countries. However, under the SSP1-2.6 scenario, the lengths of summer and winter will remain at the mid-century levels of approximately 150 and 45 days, respectively.

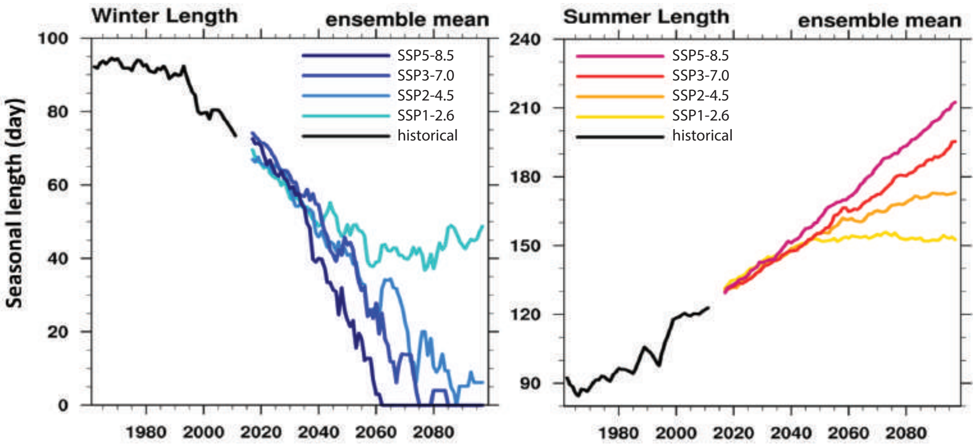

Figure 3-3

Historical simulations and projections for the lengths of winter (left) and summer (right) in Taiwan under different emission scenarios.

7. Taiwan's annual average precipitation is projected to increase slightly in the short and mid-term, with a larger increase by the end of the 21st century. Under the SSP5-8.5 scenario, the average increase is projected to reach 15%, although CMIP6 model projections estimate range from –6% to +83%, reflecting high uncertainty and low consistency. The spatial distribution of precipitation change rates exhibits low overall consistency, except in southwestern Taiwan, for which a consistent increase of 10% is projected by the end of the century under SSP5-8.5.

8. Regarding projected changes in dry and wet seasons, CMIP6 model projections indicate that Taiwan's dry season (November to April) precipitation will decrease by between 10% and 15% under the GWL of 3°C and GWL of 4°C scenarios, primarily in northeastern and eastern Taiwan, with the models exhibiting a high degree of consistency. In the wet season (May to October), precipitation is projected to increase by 5% to 15% under the GWL of 3°C. However, under the GWL of 4°C, coastal areas in central and southern Taiwan as well as Taitung and Penghu are projected to experience an increase in precipitation of more than 30% with high model consistency. Hence, the contrast between the dry and wet seasons will become more pronounced as global warming progresses.

9. Sea level rise is influenced by temperature, salinity, and density changes, and physical processes related to melting polar ice sheets and river runoff. The uncertainty in ice sheet modeling processes results in low consistency and high uncertainty in model projections of the sea level rise. Because differences in sea level changes between northern and southern Taiwan are influenced by regional ocean currents and seawater thermal structures, high-resolution numerical models are required to thoroughly investigate increases in sea level.

10. Regarding sea level, the average annual rise in Taiwan's surrounding waters was 2.2 millimeters from 1993 to 2015 (Lan et al., 2017), a rise that will persist throughout this century. Under the SSP1-2.6, SSP2-4.5, and SSP5-8.5 scenarios, the median of model projections for the sea level rise at Keelung and Kaohsiung are 0.48, 0.57 and 0.82 meters and 0.41, 0.56 and 0.78 meters, respectively, at the end of this century (source: https://sealevel.nasa.gov/ipcc-ar6-sea-level-projection-tool).

11. Projections from high-resolution atmospheric models and their dynamical downscaling data under the RCP8.5 scenario indicate a 10% decrease in typhoon frequency affecting Taiwan by the middle of the 21st century and a 50% decrease by end of the century compared with the baseline. However, the frequency of intense typhoons is expected to increase by 105% and 60%, respectively, during these periods. Maximum wind speeds are projected to increase by 5% and 9% by the middle and end of the 21st century, respectively. Additionally, typhoon rainfall intensity is projected to increase by 20% and 35% by the middle and end of the 21st century, respectively. Because of higher rainfall intensity and less frequent typhoons, accumulated typhoon rainfall is projected to increase slightly by midcentury but decrease by 10% to 50% by the end of the 21st century. The aforementioned changes are averaged values and their uncertainty spreads can be large are shown in the box plots of Figure 3-4.

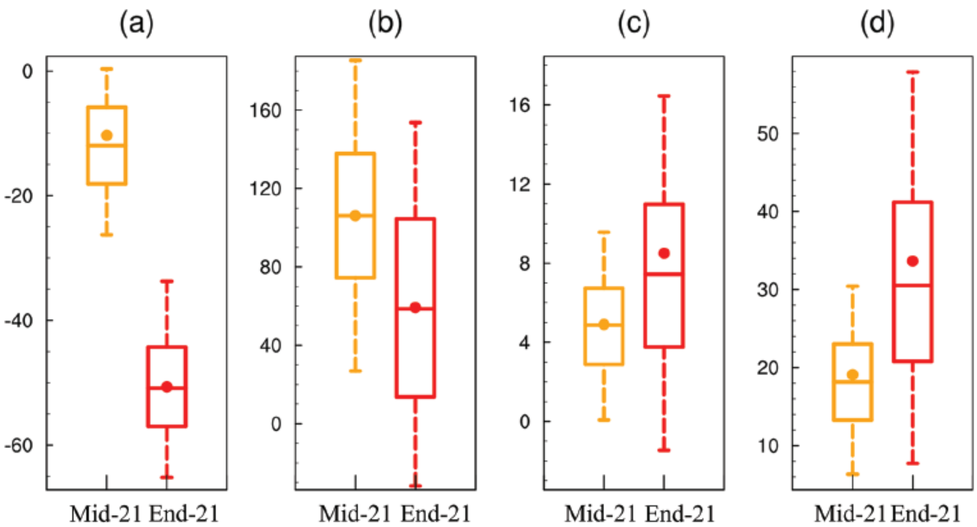

Figure 3-4

Projected changes (in percentage) of typhoons affecting Taiwan under the RCP8.5 scenario by the middle (yellow) and end (red) of the 21st century: (a) overall typhoon frequency, (b) frequency of intense typhoons, (c) maximum wind speed near typhoon centers, and (d) average rainfall within 200 km of typhoon centers (adapted from Cheng et al., 2024).

12. Regarding extreme climate events, an increasing trend is projected in the maximum number of CDDs associated with droughts. This trend will become more pronounced toward the end of this century as warming intensifies, with southern Taiwan experiencing a more severe increase than northern Taiwan.

13. Long-timescale drought events (SPI12) indicates that, as warming intensifies, drought events will become less frequent and shorter duration across Taiwan by the end of this century. Short-timescale drought events (SPI3) will increase in both intensity and frequency.

14. Projections suggest a decreasing trend in spring precipitation, likely due to weakening of the low-level southwesterly flow, which provides moisture, and a northward shift of the East Asian front.

15. The number of extremely hot days (annual count of days with daily maximum temperatures equal to or above 36°C) will increase by 4.7, 9.7, 26.7, and 53.5 days under GWL of 1.5°C, 2°C, 3°C and 4°C, respectively. Under the worst-case SSP5-8.5 scenario, the median increase will be 73.6 days by the end of this century. Larger increases in hot days will include the Taipei Basin, near the mountains area from central to south Taiwan, particularly in valleys (river valleys and longitudinal valleys), due to a lack of sea breeze regulation and closed terrain (Figure 3-5).

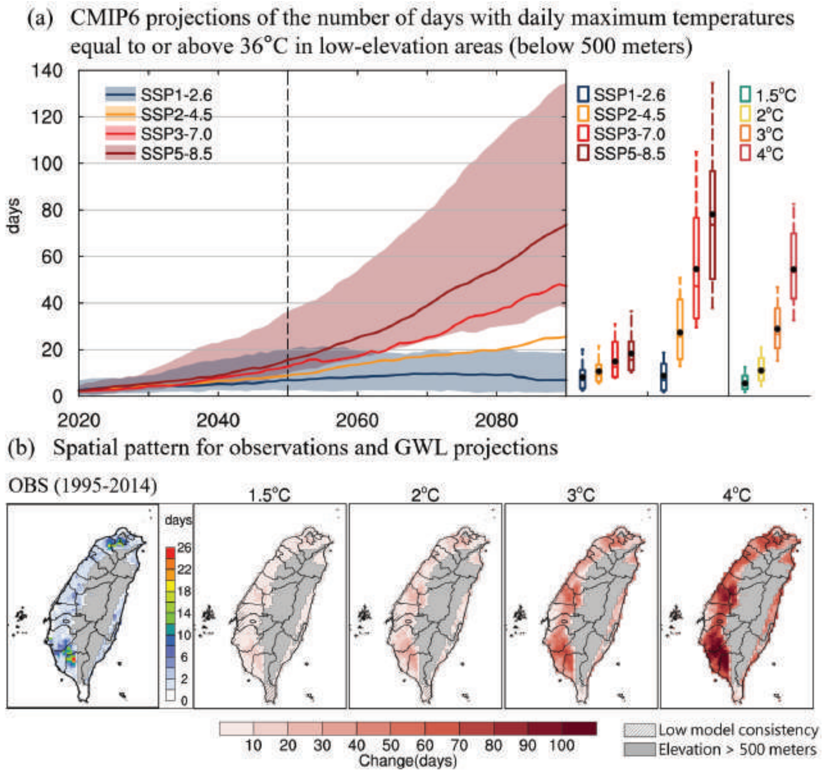

Figure 3-5

(a) CMIP6 projections of the annual count of days with maximum temperature equal to or above 36°C in low-elevation areas (below 500 meters) with different emission scenarios and (b) the spatial distribution from observation during baseline period and GWL of 1.5°C, 2°C, 3°C and 4°C

16. The number of extremely cold days (Cold Wave Duration Index, CWDI) will decrease under all warming scenarios. In the four GWLs (GWL of 1.5°C, 2°C, 3°C and 4°C), the average expected decrease is 4.1, 6.6, 8.8, and 10 days per year, respectively. However, the probability of being affected by cold surges is low because Taiwan is located in the subtropics. Low consistency and high uncertainty affect the multimodel projections.

17. In terms of afternoon convection during summer, model projections under the high-warming scenario (RCP8.5) suggest that warming will lead to an increase in atmospheric vertical stability, which is unfavorable for the occurrence of afternoon convection and will lead to a decrease in rainfall frequency by the end of the 21st century. However, the stronger southwesterly flow and low-level convergence induced by the enhanced Pacific subtropical high is favorable for the oceanic precipitation system to move towards Taiwan. Following this, the increases in low-level water vapor over Taiwan and adjacent areas will intensify rainfall once precipitation is triggered.

18. By the projection in the end of the 21st century under the high emission scenario (RCP8.5), the number of days with extreme rainfall and the intensity of these events increased on the windward side of western Taiwan during the Meiyu season but decreased in eastern Taiwan.

19. In the mid-to-late 21st century (after 2060), under the SSP3-7.0 scenario, model projections indicate that Meiyu season rainfall will be delayed from late-May to late June and that rainfall intensity will increase. This phenomenon may be related to a delay in the strengthening of the southwest monsoon in the South China Sea, causing a delay in the occurrence of intense rainfall in downstream Taiwan.

20. Over the past century, rainfall changes in Taiwan have not been significant. Projections under warming scenarios do not reveal consistent changes in rainfall because of the high uncertainty between models. However, the difference between the dry (November to April) and wet (May to October) seasons increased with the increasing GWL. For example, during the dry season, most regions in Taiwan are projected to experience reduced rainfall, especially the northeastern and eastern areas. Additionally, under GWLs of 1.5°C and 2°C, model projections indicate an increase in the number of dry days (albeit with low model consistency) in the southwestern region, which is typically dry.

21. Under GWL of 4°C, wet-season rainfall is projected to increase notably across Taiwan with high model consistency. Rainfall in the coastal areas of central and southern Taiwan, in addition to Taitung and Penghu, could increase by more than 30%. These results suggest that with more severe global warming, the trend in Taiwan's seasonal rainfall pattern—of the dry season becoming drier and the wet season becoming wetter—will become more pronounced. (Figure 3-6)

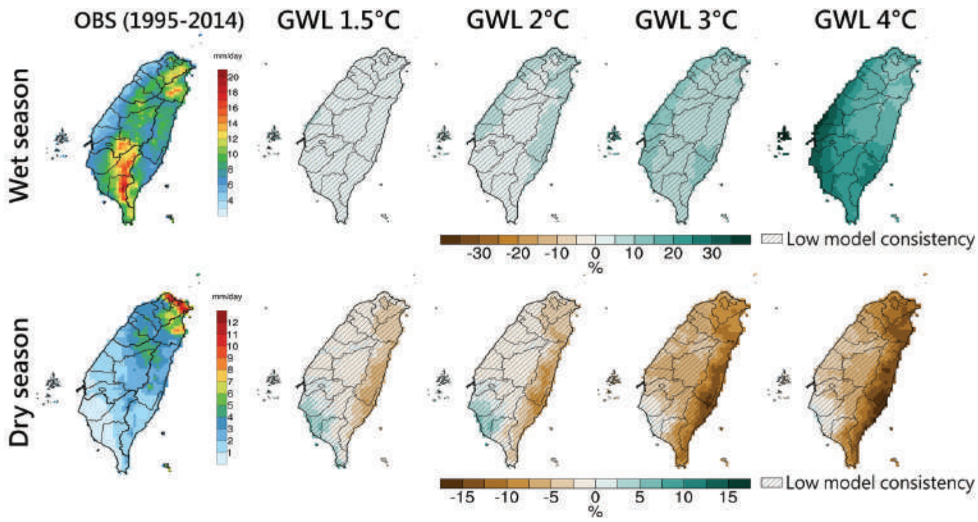

Figure 3-6

Observed mean rainfall and projected changes under various GWLs in Taiwan during the wet (top) and dry (bottom) seasons

22. The intensity of the yearly maximum 1-day precipitation (Rx1day) is projected to increase as global warming intensifies, especially in central Taiwan under the SSP5-8.5 scenario, where the increase may reach 40%.

23. Under warming scenarios, the trend in Taiwan's rainfall is characterized by "precipitation polarization"; the projection of maximum number of CDD increased as the annual frequency of heavy rainfall events. For example, by the end of this century, springtime CDD across Taiwan increased in number under all emissions scenarios. The southern regions—such as Chiayi, Tainan, Kaohsiung, Pingtung, and Taitung—which experienced longer dry periods in spring.

24. The results of an analysis of the 10-year and 50-year return periods of rainfall intensity reveal that under GWL of 4°C, the 10-year return period rainfall intensity is 468 millimeters, which is the intensity of 50-year return period in present climate. This shift may pose considerable challenges to flood and slope stability management (Figure 3-7).

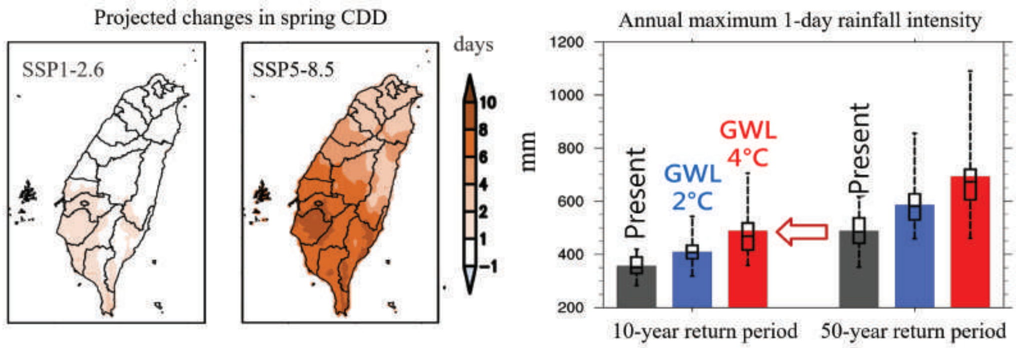

Figure 3-7

(left) Projected changes in number of CDD for spring by the end of the 21st century under warming scenarios (units: days/year; adapted from Chen et al., 2023) and (right) average annual maximum 1-day rainfall intensity for Taiwan under various GWLs.

25. The results of a hydrological frequency analysis indicate that when warming reaches 4°C, rainfall intensity that currently occurs once every 50 years will occur once every 10 years, revealing that extreme rainfall will have increasingly severe impacts on Taiwan.

26. Under the GWL of 2°C and GWL of 4°C scenarios, with emissions held constant, Taiwan's air quality is projected to worsen, with more pronounced degradation in autumn and winter compared to spring and summer.

27. The primary driver of this decline is the weakening of low-level winds under warming conditions, which restricts pollutant transport and dispersion. However, localized factors, such as increased autumn rainfall in southwestern Taiwan, may partially mitigate these effects.

28. The key pollutants contributing to poor air quality are fine particulate matter ($PM_{2.5}$) and ozone (O_3). Ozone exhibits a stronger response to warming than $PM_{2.5}$. Rainfall has a minimal effect on removing gaseous pollutants, while elevated temperatures accelerate photochemical reactions, leading to higher ozone concentrations. (Figure 3-8).

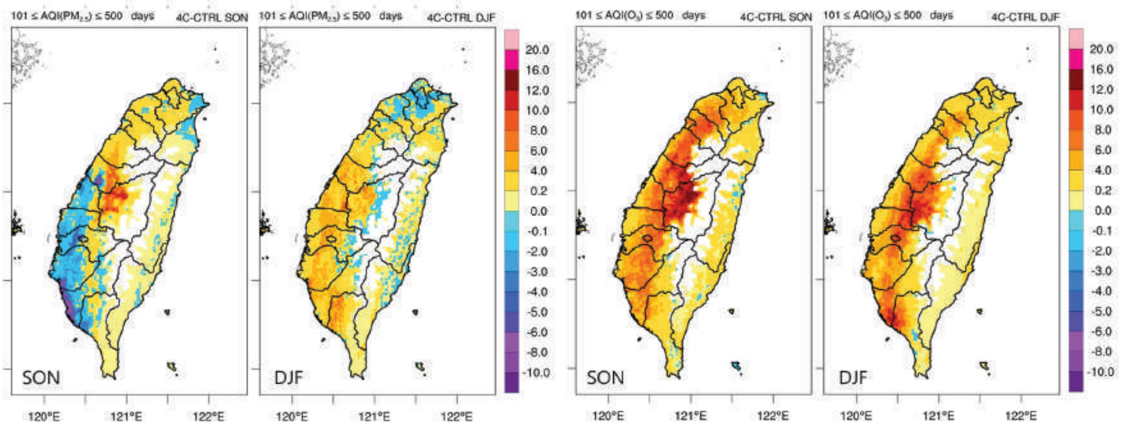

Figure 3-8

Simulated changes in the number of days with poor air quality due to $PM_{2.5}$ (left two panels) and ozone (right two panels) during autumn (September–November, SON) and winter (December–February, DJF) represent the differences between the GWL of 4°C scenario and the historical period. The left two panels are adapted from Tsai et al. (2024).

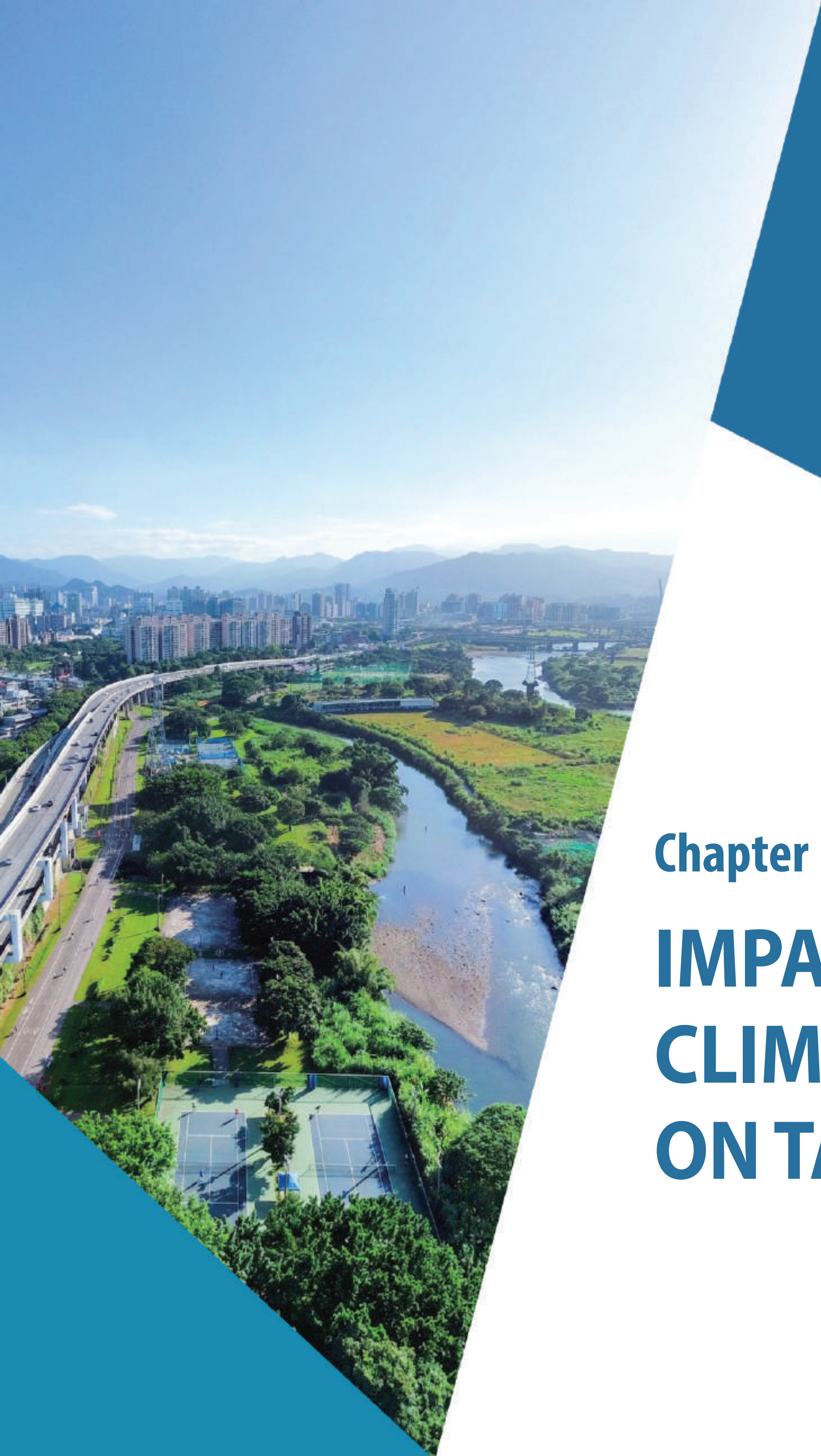

Chapter 4

IMPACTS OF CLIMATE CHANGE ON TAIWAN

4.1 Water

1. This Report's flooding risk assessment used hourly rainfall projections from the IPCC AR5 RCP8.5 scenario. The overall size of flood-prone areas will increase during the middle and by the end of the century. Approximately 14% of Taiwan's towns will be at higher flood risk, and 3% of cities will face more severe flooding due to climate change. Flood prevention plans should target more vulnerable areas to reduce flood risks (Chen et al., 2022).

2. An inundation depth of 0.5 meters and above is employed as an indicator to evaluate the probability of flooding, which is presented on a color scale from light blue (low) to dark blue (high) (Figure 4-1). The results of the analysis indicate that the overall area affected by flooding will increase by approximately 1.2 times by the middle of the century compared with the base period and increase by approximately 2.3 times by the end of the century. These results demonstrate that both the probability and scale of flooding will increase.

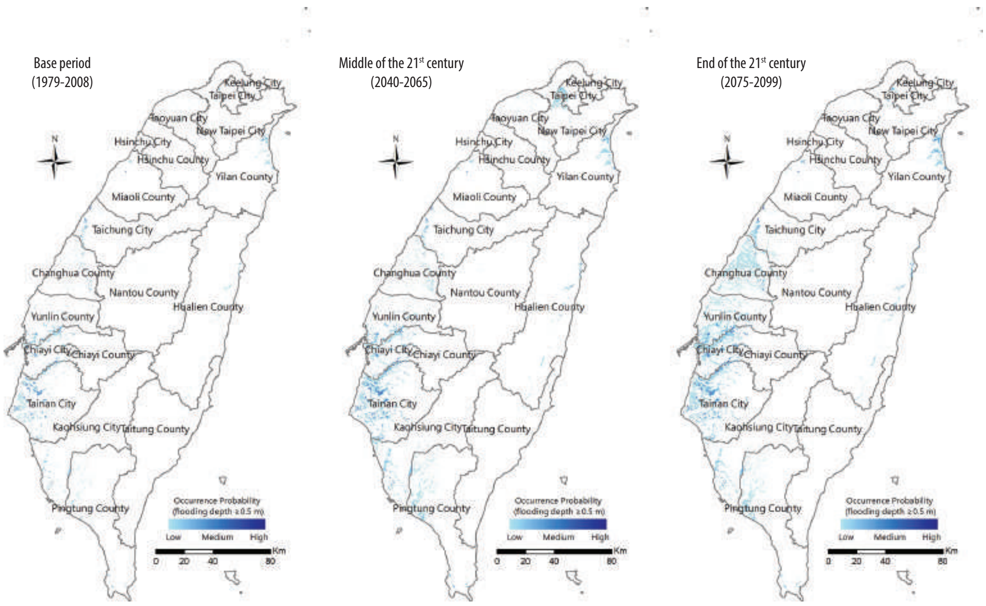

Figure 4-1

Probability and Distribution of Flood Events (Flooding Depth ≥ 0.5 m)

3. The number of CDDs is projected to increase under several climate change scenarios. For example, under the GWL 2°C scenario, the number of CDDs in northern, central, and southern Taiwan could increase by 16.9%, 11.1%, and 13.7%, respectively, leading to longer periods without rainfall. Low-flow discharge (Q85) in northern, central, and southern Taiwan is projected to decrease consistently. In the most severe scenario, reductions in low-flow discharge are expected to range from –18.2% to –49.5%. Additionally, an increased probability of delayed Meiyu season and delayed typhoon conditions are anticipated. Consequently, hydrological conditions are expected to trend toward more frequent extreme events (Figure 4-2).

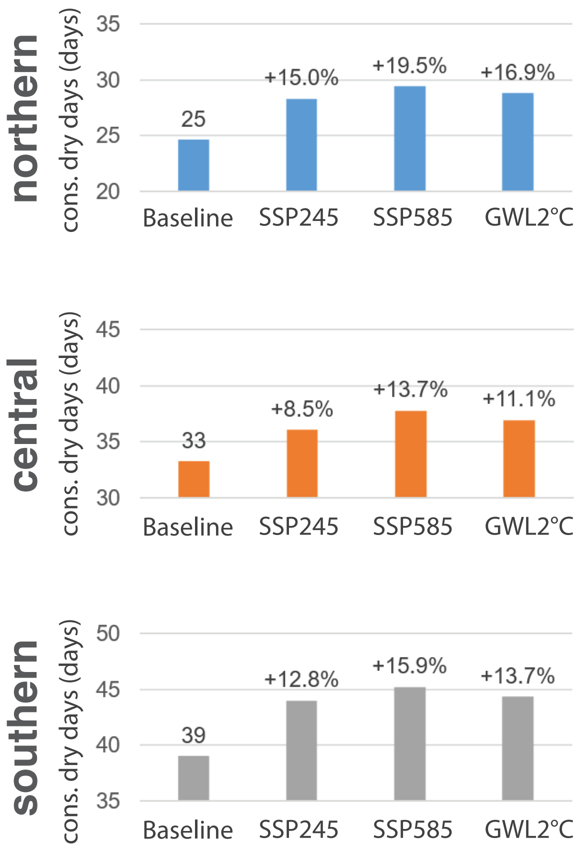

Figure 4-2

Changes in CDDs under Various Climate Change Scenarios

4. Taiwan's annual rainfall is 88.502 billion tons, although this abundance is unevenly distributed. After deducting losses due to evapotranspiration and runoff into the sea, the annual runoff volume is approximately 64.742 billion cubic meters. Since 2017, several studies in Taiwan have used AR5 or AR6 data to simulate changes in rainfall or runoff under various climate change scenarios. This Report conducted a comprehensive analysis of AR5 and AR6. The results of the analysis demonstrate that the annual runoff will vary between –1% and +27%. Using the latest AR6 data to simulate flow rate changes under GWL 2°C and GWL 4°C, the median of the multiple results indicate that the annual flow rate change across Taiwan will range from –1% to +27%. In the wet season, the flow rate change will range from –2% to +31%, whereas in the dry season, the change in flow rate will range from –13% to +3%. This wide variation will increase the difficulty of water resource allocation (Figure 4-3).

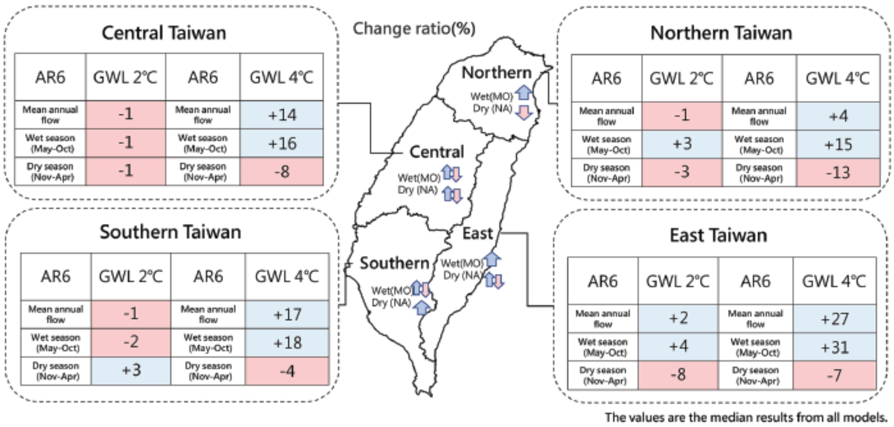

Figure 4-3

Rate of Flow Changes Under the impacts of Climate Change (%)

Note: The values in the table represent the median of all models (ranging from the 5th percentile to the 95th percentile). The GWL 2°C and GWL 4°C scenarios refer to the periods when global temperatures warm by 2°C and 4°C, respectively, and were compared with the baseline period (1995–2014). The number of models used was 86 for GWL 2°C and 26 for GWL 4°C. Because various models reach the GWL 2°C or 4°C at different times, the reference periods for GWL 2°C and GWL 4°C are between 2041–2060 (middle term) and 2081–2100 (long term), respectively. Runoff simulation is a nonlinear hydrological process influenced by different hydrological fluxes, such as evapotranspiration and groundwater outflow, which can cause the range of runoff changes to differ from that of precipitation changes.

5. Under the AR5 RCP8.5 scenario, the current water supply in northern Taiwan may decrease by between 3.3% and 6.0%; that in central Taiwan, by between 3.9% and 4.3%; and that in southern Taiwan, by 2.7%. Eastern Taiwan may have unstable water supply during the dry season and high turbidity during the wet seasons. Regarding changes in groundwater, results under the AR4 A1B scenario indicate that groundwater levels in the nine groundwater regions could decrease by between 19.6% and 54.6% or increase by between 20.9% and 48.1%.

6. Water-related challenges must be addressed by multiple ministries and agencies, and climate change adaptation strategies will require cross-sectors collaboration or integrated management approaches. Assessing the water demand of various sectors and allocating resources accordingly will be crucial. Using scientific data as an evidence-based foundation for formulating national water resource management strategies will ensure that the co-benefits of various adaptation options are maximized, optimizing water resource efficiency and reducing the impacts of climate change.

4.2 Slopes

1. Under the AR5 RCP8.5 scenario, the average landslide-area ratio of the baseline period in the northern region ranges from 0.16% to 0.47%, increasing to 0.23% to 0.77% by the end of the 21st century. This difference reveals a trend of escalating landslide risks in the northern region due to climate change.

2. Under the AR5 RCP8.5 scenario, the average landslide-area ratio of the baseline period in the central region ranges from 1.3% to 3%, rising to between 1.4% and 4% by the end of the 21st century and exhibiting an overall increase in the influence of landslides.

3. The average landslide-area ratio of the baseline period in the southern region is between 1.7% and 2.9%, which is projected to increase to 3.2% by middle of the 21st century and decrease to 1.3% by the end of the 21st century.

4. Chen et al. (2024) combined AR6 statistical downscaled precipitation data, geomorphological characteristics of slopes, and population density to assess landslide risks in Taiwan under various levels of global warming. At GWL 2°C, the landslide risks in central and southern Taiwan are high, with increased risk also expected in the northern and eastern mountainous areas; if warming rises to 4°C, the risk in some mountainous areas increases substantially (Figure 4-4).

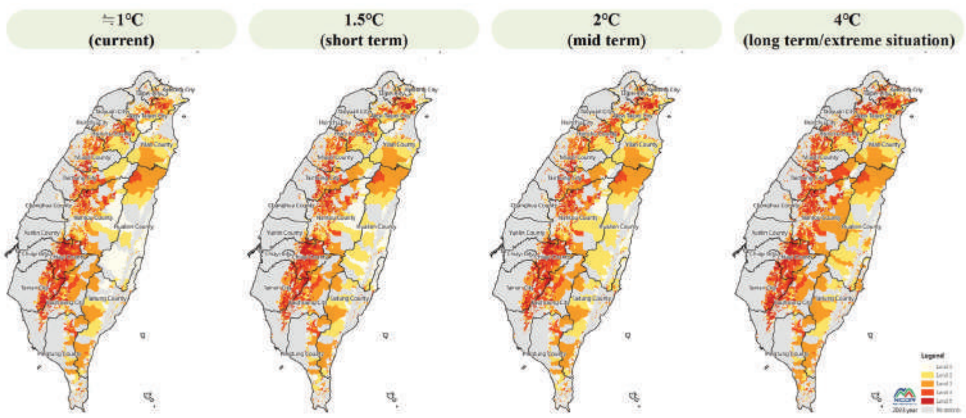

Figure 4-4

Landslide Risk within Basic Statistical Areas under Various GWLs (Source: Chen et al., 2024)

4.3 Coastal Area

1. The IPCC AR6 projections indicate that under GWLs of 1.5°C and 2.0°C, sea levels in Taiwan will rise by 20cm and 34.5cm, respectively.

2. Coastal flooding in Taiwan, primarily caused by sea level rise, will extend further inland and be deeper under GWL 2.0°C than under GWL 1.5°C. Inundation area percentages for coastal counties and cities range from 0.08% to 2.71% under GWL 1.5°C and increase to between 0.30% and 4.30% under GWL 2.0°C. Yunlin County has the largest inundation area percentage under both scenarios. The maximum flooding depths in New Taipei City, Changhua County, Yunlin County, Chiayi County and City, and Taitung County exceed 1.5 meters under GWL 1.5°C. Additionally, the maximum flooding depths in Taoyuan City, Hsinchu County and City, Tainan City, Kaohsiung City, and Hualien County exceed 1.5 meters under GWL 2.0°C (Figure 4-5).

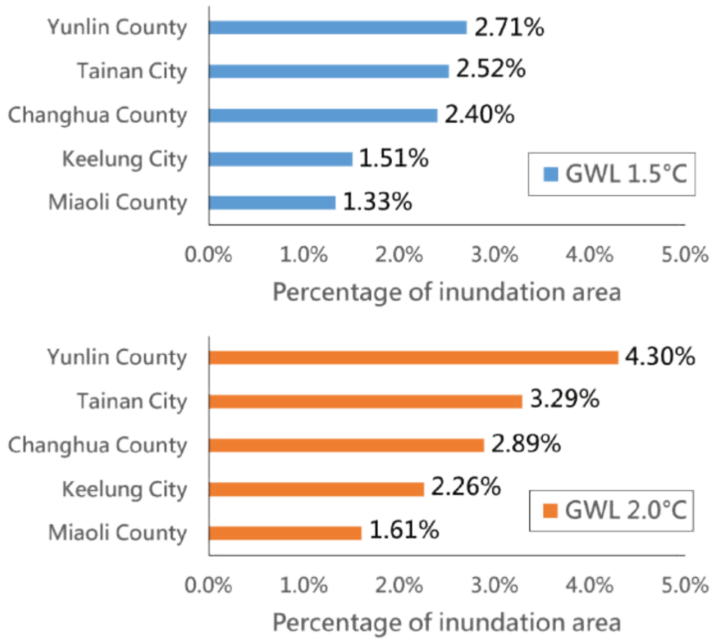

Figure 4-5

The top five counties and cities in Taiwan ranked by the percentage of inundation area

3. By the end of the 21st century, under AR5 RCP8.5 scenario, the length of coastline affected by typhoon surges exceeding 1.2 meters will increase by 12.5%, whereas the coastline exposed to typhoon waves over 12.0 meters will increase by 3.6%.

4.4 Food Security

1. Taiwan's food self-sufficiency rate, calculated using caloric intake, has declined from 43% in 1990 to 31% in 2021.

2. Peng et al. (2004) suggest that a warming climate may lead to a 10% to 15% reduction in yields in Asia's major rice-producing regions. Specifically, a 1°C increase in nighttime temperature during the dry season will reduce yields by 10%; for daytime temperature between 28°C and 34°C, each 1°C increase in temperature will cause a yield loss of between 7% and 8%.

3. Taiwanese and international studies have indicated that climate change has adversely aected crop yields and caused economic losses. The TCCIP team employed the Decision Support System for Agrotechnology Transfer (DSSAT) crop growth model, integrating climate projection data to assess the projected changes in rice and corn yields in Taiwan to facilitate analysis under the high-emissions global warming scenario RCP8.5. The overall trend is a decline in rice yields, with reductions of 13% and 18% by the middle and end of 21st the century, respectively. Similarly, corn yields are expected to decline, with average reductions of 10% and 17%, respectively, with the most substantial changes occurring in northern and eastern Taiwan (Figure4-6).

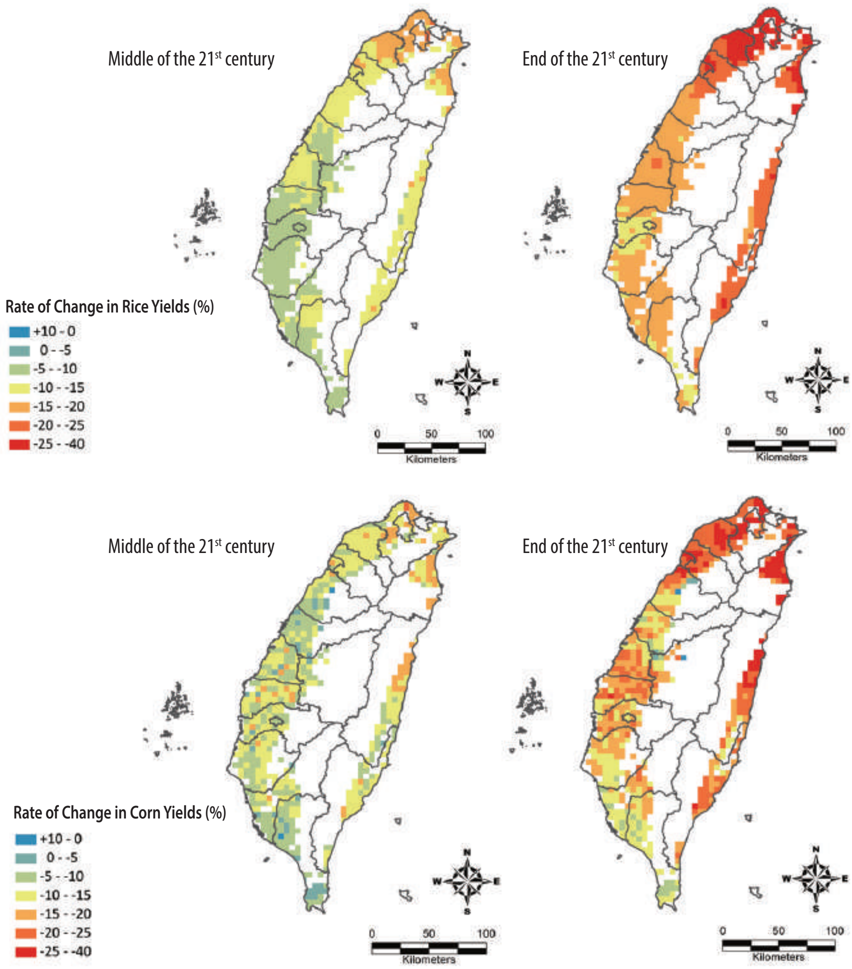

Figure 4-6

Rates of Change in Rice and Corn Yields under Climate Scenario RCP8.5

4. Changes in the temperature–humidity index (THI) under the AR5 RCP 8.5 scenario at GWL 2°C and GWL 4°C indicate that areas experiencing livestock heat stress (THI ≥ 72) will fall within the red alert zone, which is projected to expand progressively from the southern to northern regions and from the lowland plains into foothill areas (Figure 4-7).

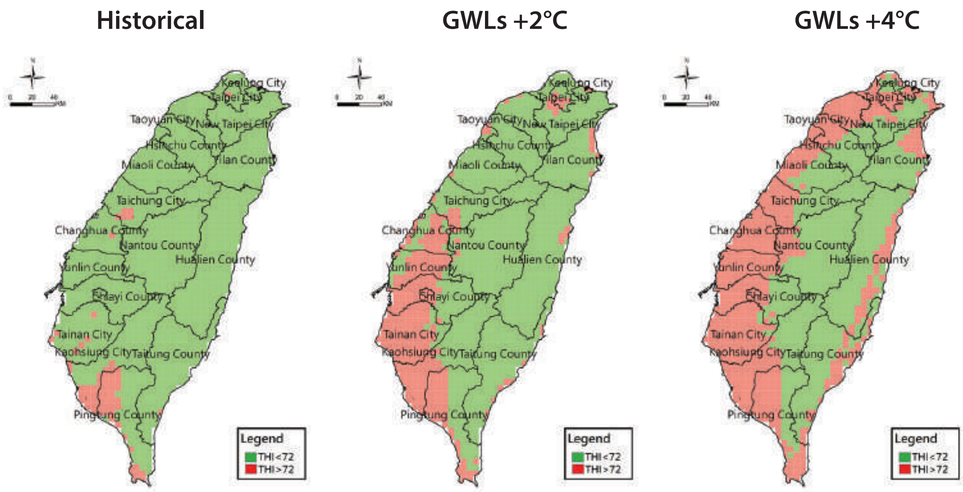

Figure 4-7

Trends in THI in Taiwan under Climate Change

5. Since 2010, long-term climate change and extreme climate events have disrupted the aquaculture industry, causing environmental degradation and sudden species loss, leading to operational losses for fishermen.

6. This study used extreme temperature event data under the AR6 GWLs (GWL 1.5°C and GWL 2°C) scenario published by the TCCIP in 2023 to simulate and analyze climate hazards and exposure to Chanos chanos and *Meretrix lusoria (M. lusoria)* aquaculture. Low oxygen levels and water quality deterioration directly or indirectly affect the production of *M. lusoria*. Through document analysis, this study identified hazards involved and approaches for adapting to these hazards, mapping two indicators of national adaptation scenarios defined in the National Climate Change Action Guidelines (2023–2026) and conducting in-depth interviews with stakeholders. The results reveal that although identical challenges *are faced by M. lusoria* aquaculture areas in various Taiwanese towns, the hazard and risk exposure vary from town to town (Figure 4-8).

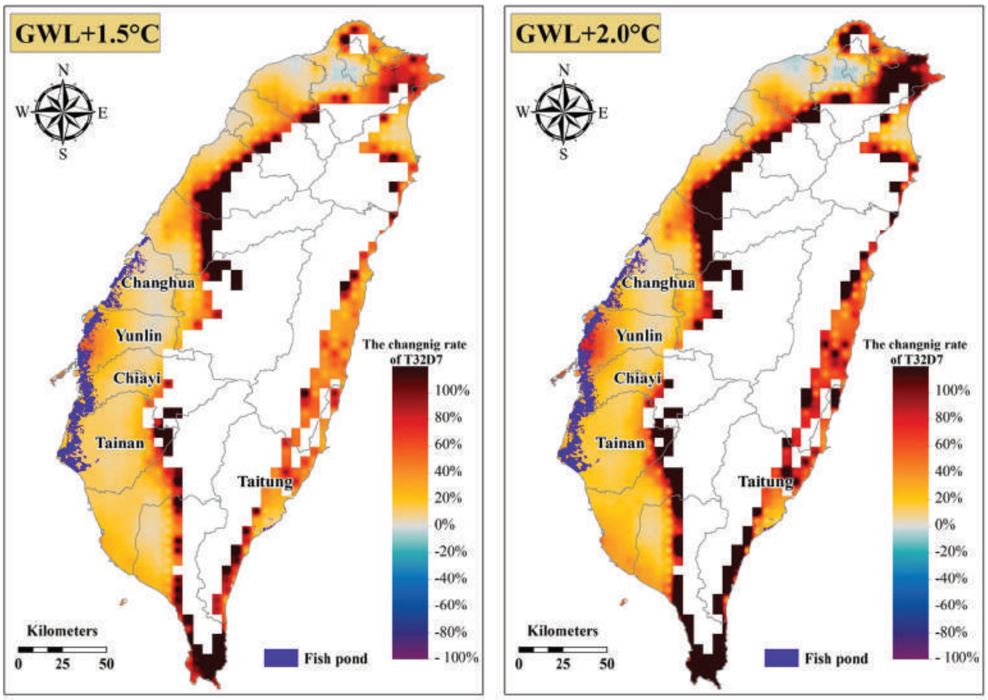

Figure 4-8

Changing Rates of High-Temperature Hazards to the M. lusoria Aquaculture Industry under AR6 GWLs (GWL 1.5°C and GWL 2°C)

7. From 2014 to 2019, the gray mullet *(Mugil cephalus Linnaeus)* gradually shifted its primary fishing location northward due to the effects of climate change on the fishing ground environment.

8. The fishing habitat for *Uroteuthis. edulis (U. edulis)* (commonly known as the swordtip squid) in Taiwan has historically been centered around the Pengjia Islet, where the average sea temperature is 25°C. The Fisheries Research Institute used climate projection data from the TCCIP under the AR6 emission scenarios SSP1-2.6 and SSP2-4.5 to conduct a catch survey for *U. edulis*. The study discovered that when the sea temperature increased by 1°C, the catch per unit effort for *U. edulis* decreased by 15%. However, under the SSP1-2.6 mitigated emission scenario, the suitability of the habitat for *U. edulis* around Taiwan's Three Northern Islands and near the waters at 30°N latitude increases (Figure 4-9).

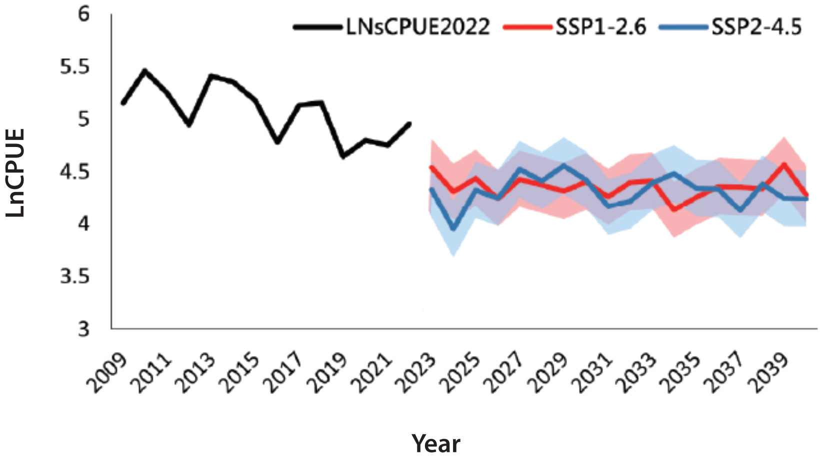

Figure 4-9

Trends in U. edulis catches in 2040 under the SSP1-2.6 and SSP2-4.5 scenarios

9. The Sakura shrimp (*Sergia lucens*) is a crucial species in the southwestern waters of Taiwan. Its survival is strongly affected by water temperature, which should ideally range from 11°C to 25°C. An analysis of the data from 2005 to 2019 reveals a decline in the catch of Sakura shrimp in Donggang township, likely due to changes in the marine environment affecting shrimp distribution.

4.5 Ecology

1. Taiwan's forests are classified into 21 types according to the National Vegetation Survey and Mapping Project conducted in 2013. This survey revealed that 14 forest types are highly sensitive to climate change and exhibit wide zonal distributions that are strongly affected by temperature and rainfall gradients. These forest types reflect the representative vegetation composition and structure under Taiwan's natural environmental conditions. The remaining forest types are azonal and influenced by regional factors such as succession, forest fires, landslides, elevated coral formations, riverbanks, and karst topography (Li et al., 2013).

2. Climate change affects the growth rates and reproductive success of several species, potentially driving populations or individuals to migrate in search of more suitable habitats. Species or populations that cannot rapidly relocate to more appropriate environments or develop more adaptive behaviors may be at risk of extinction.

   A species distribution model for subalpine woodlands and shrubs revealed a substantial decline in suitable habitat, ranging from 16.08% to 2.58% under RCP 4.5 and RCP 8.5 scenarios, with a potential upward shift from 173 to 268 meters (Lin, 2020). High mountain peaks, characterized by cold, windy, and barren conditions with little to no soil, are harsh environments that hin der plant growth. These factors may accelerate the population decline and extinction of alpine plants (Figure 4-10).

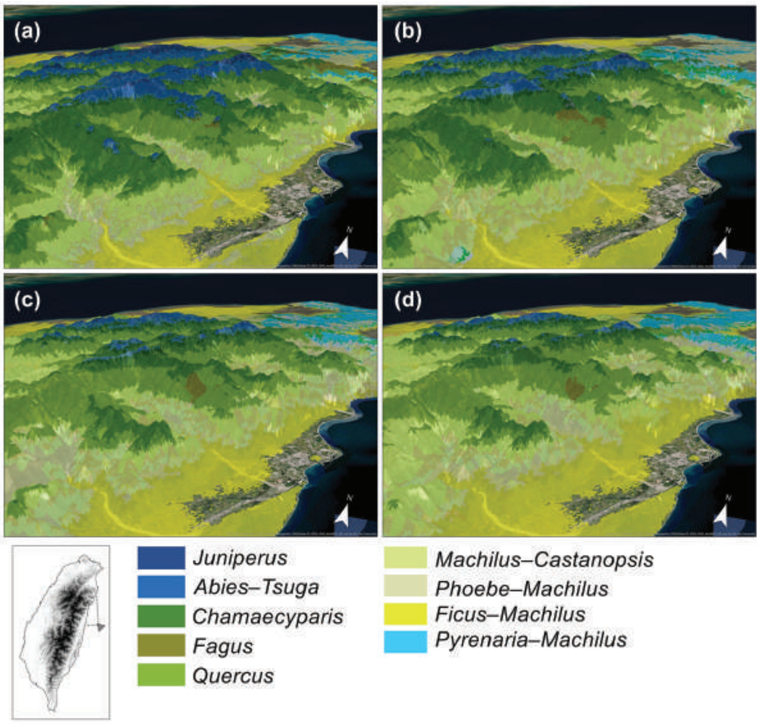

Figure 4-10

Simulated Coverage for Various Forest Types under the AR5 Scenarios

Note: (a) Baseline period of 1986–2006, (b) 2030–2040, (c) 2060-2070, and (d) 2090–2100. The simulation reveals a distinct decline in the range of high-mountain forests, indicating that alpine and subalpine areas could be highly affected by climate change.

3. Wang (2019) evaluated the vulnerability to climate change of 83 breeding bird species in Taiwan, revealing 41 species are under high climate change risks. Furthermore, 16 and 22 species are sensitive to temperature and rainfall, respectively. Due to a combination of diet, nursing, and other factors, 46 of these bird species are relatively unable to cope with the impacts of climate change.

4. Climate change can potentially reduce the habitat and population of endemic species in high-altitude areas. For example, Bombus formosellus, an endemic bumblebee found at high elevation, thrives in conifer forests and grasslands but is less suited to broadleaf forests, mixed forests, farmland, and developed areas. Simulations under warming scenarios from RCP 2.6 to RCP 8.5 predict shrinkage of the suitable habitat for this bumblebee by 41% to 87%. Consequently, viable habitats for the species in southern Taiwan may soon cease to exist (Lu & Huang, 2023).

5. A distribution model for the Taiwan fir (Abies kawakamii) and the Taiwan hemlock (Tsuga chinensis) predicts that the suitable range for these conifer species will shift upward in nearly half of the 15 AR4 scenarios (Lin et al., 2014).

6. A study on the Taiwan beech (Fagus hayatae) under the RCP4.5 and RCP8.5 scenarios suggests that by 2100, the remaining suitable habitat for this beech will be reduced to just 7.1% or 0.87% of its current range (Lin, 2020). The highly topographically isolated populations of Taiwan beech limit the species' ability to migrate, potentially leading to local extinction. On-site population monitoring has revealed trends consistent with these predictions, indicating that Taiwan's beech forests may be among the most vulnerable to climate change.

7. Climate change may alter competition behaviors between animal species of the same trophic level. An experiment investigating competition between larvae of two scavengers, the burying beetle (Nicrophorus nepalensis) and the blowfly, revealed that the food resource competition behavior of these two species changes along the elevation (temperature) gradient. At low elevation (high temperature), food searching times are shorter for both species, and increased clutch size leads to faster decay of food, adversely affecting the breeding rates of the burying beetle (Chan et al., 2019).

8. The potential impacts of climate change continue to develop. In the Taiwan Strait, a rapid warming trend of 0.63°C over the decade since 2012 suggests that the hiatus in the increase of SSTs from 1998 to 2011 did not continue from 2012 (Lee et al., 2021). Increasing SSTs may change the vertical profile and horizontal distribution patterns of seawater temperatures, leading to changes in habitation environments of numerous aquatic organisms.

9. Per McRae et al. (2022), corals in southern Taiwan can tolerate chronic warming above seasonal mean temperatures. Nevertheless, bleaching can occur after acute exposure to a temperature 2°C above the mean summer maxima. Additionally, coral undergo substantial bleaching (50%–100% of all nubbins) upon exposure to acute short-term elevated temperature conditions (8 days at 32°C).

10. Lee et al. (2022) indicated that the total catch of mackerel, squid, hairtail, and dolphin fish is strongly correlated with the North Pacific Gyre Oscillation. Total catches for these fish under the RCP 8.5 scenario may decrease by 2.41% from their 2020 levels.

11. The new-generation Earth system model outputs from Phase 6 of the CMIP6 suggest a greater decline in mean global ocean animal biomass under both strong-mitigation and high-emissions scenarios due to elevated warming (Tittensor et al., 2021). CMIP6 models predict larger declines in marine animal biomass after 2030, with almost every year exhibiting a pronounced decrease under strong mitigation and most years from 2060 onwards exhibiting a catastrophic decrease under high emission scenarios (Figure 4-11).

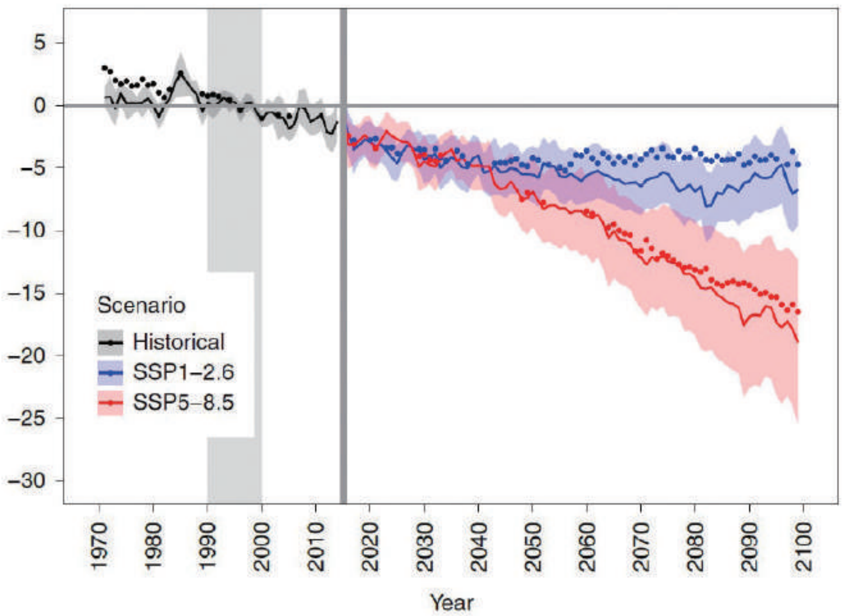

Figure 4-11

Multimodel Mean Changes in Marine Animal Biomass under Strong-Mitigation and High-Emissions Scenarios

Note: Blue coloring represents strong mitigation, and red represents high emissions.

4.6 Health

1. Extreme temperature affects cardiovascular health by increasing aortic blood pressure (Hintsala et al., 2014). The effects of extreme heat on health are immediate, whereas extreme cold exerts delayed effects (Chung et al., 2015). Climate change has increased daily temperature variability, defined as the difference between the maximum and minimum temperatures. Kim et al. (2016) revealed that every 1°C increase in temperature variability increases the risk of death from cardiovascular diseases by 0.81% and from respiratory diseases by 0.90%.

2. International research reveals a strong association between high temperature and increased mortality risk from cardiovascular and respiratory diseases among the Taiwanese population (Chung et al., 2017). Additionally, a separate analysis of mortality data from 567 cities in 27 countries across five continents uncovered a positive association between extreme temperature and cardiovascular deaths. Specifically, for every 1,000 deaths, 2 were attributed to extreme heat and 9 to extreme cold (Alahmad et al., 2023).

3. Climate hazards can worsen pathogen transmission. For example, higher temperature results in faster spread of vector-borne diseases such as dengue and chikungunya by influencing mosquito spread, underscoring the ability of climate events to intensify disease transmission through specific transmission routes (Mora et al., 2022).

4. Floods indirectly increase the risk of waterborne diseases. Human contact with contaminated water and animal waste (Suk et al., 2020) and cohabitation with rodents in evacuation areas elevate the risk of leptospirosis (Watson et al., 2007). Additionally, when daily rainfall exceeds 80 mm during typhoon season, the incidence of shigellosis can double (Chen et al., 2022).

5. The risk of death from chronic lung disease during heatwaves is between 1.8% and 8.2% higher than that under average summer temperatures (Witt et al., 2015). High indoor temperatures worsen symptoms such as shortness of breath, coughing, and sputum production in patients with moderate to severe chronic obstructive pulmonary disease (COPD) (McCormack et al., 2016).

6. Research links increased air pollution to increased risks of allergic conjunctivitis (AC) and allergic rhinitis (AR) (Hsieh et al., 2020; Zhong et al., 2019). NO_2, O_3, and temperature variations are correlated with conjunctivitis, whereas rhinitis is primarily linked to NO_2 levels.

7. Allergens in green spaces may increase the risk of AR in children by 8.4%. Fluctuations in outdoor temperature and humidity also contribute to AR. Increased concentrations of PM10, PM2.5, and NO_2 worsen lung function, reduce blood oxygen saturation in patients with COPD, and exacerbate emphysema severity (Tran et al., 2022).

8. Kim et al. (2019) analyzed urban data from 341 regions across 12 countries and revealed that high environmental temperature is associated with an increased risk of suicide. Data from the United States and Mexico also reveal a linear relationship between temperature and suicide rate; specifically, for every 1°C rise in the average monthly temperature, the suicide rate was found to increase by between 0.68% and 2.1% (Burke et al., 2018).

9. Chen et al. (2019) investigated long-term exposure to extreme temperature in Taiwan and discovered that in regions where the annual average temperature exceeds the median of 23°C, each additional 1°C increase in temperature leads to approximately a 7% increase in the incidence of major depressive disorder. This effect is most pronounced in individuals aged 65 years or older.

10. Lung et al. (2018) identified four crucial areas for research on health adaptations to climate change: developing comprehensive early warning systems for health impacts, investigating cobenefits health strategies that mitigate the impacts of climate change and improve health, creating health promotion tools, and strengthening research on climate and health adaptation. The most urgent priority is establishing a predictive model for assessing climate-related adverse health impacts.

11. Lung et al. (2018) synthesized the literature (Table 4-1) and categorized the types of climate conditions affecting health into three groups: temperature variation, precipitation variation, and combined temperature and precipitation variation.

Table 4-1 Adverse Health Impacts Associated with Climate Change

Climatic Characteristics	Physical Conditions	Adverse Health Impacts
Temperature variation	Extreme high temperature	Dehydration Increased total cardiovascular disease incidence and mortality rate Atrial fibrillation Increased prevalence of ischemic heart disease Increased myocardial infarction morbidity and mortality rates Increased visits for heatstroke Increased prevalence of ischemic stroke Increased total respiratory disease incidence and mortality rate Increased prevalence of COPD Adverse effects on mental health
	Extreme low temperature	Increased total cardiovascular disease mortality rate Increased total respiratory disease incidence and mortality rate
Precipitation variation	Waterborne diseases	Ocular infections Respiratory tract infections Gastrointestinal diseases Allergic dermatitis Varied seasonal and geographical distribution of infectious diseases
Combined temperature and precipitation variation	Temperature and humidity variation	Vector-borne disease (Malaria [Anopheles mosquito], dengue fever [Aedes albopictus and Aedes aegypti], Japanese encephalitis [Culex tritaeniorhynchus Gile, Cx. annulus Theobald and Cx. fuscocephala Theobald])

4.7 Urban and Rural Spaces

1. Urban expansion in densely populated areas requires the integration of climate science with key findings from the humanities and social sciences. Practical strategies must incorporate risk, vulnerability, and adaptation planning theories to evaluate and manage the risks posed by climate change. This approach is crucial for ensuring sustainability in urban and rural areas.

2. Research on disaster vulnerability under long-term climate and spatial change scenarios and the link between risk reduction and adaptation need more exploration. This Report recommends integrating spatial analysis of land use changes with vulnerability assessments for proactive adaptation planning. Such an approach can help evaluate adaptive capacity under projected scenarios and enable dynamic adjustments to urban development, land use, and adaptation strategies, reducing the disaster risk and avoiding maladaptation.

3. In Taiwan, slope risk assessments have established indicators and spatial formats for climate-related disasters, but these focus primarily on disasters under current conditions. Future research should address landslide hazards under climate change to inform adaptation strategies and improve resource allocation by identifying vulnerability hotspots across time and space.

4. Effective adaptation requires integration of climate change projections into national spatial planning for the farmland. This approach must account for interactions between surrounding land and socioeconomic activities, balancing agricultural production with ecosystem services.

5. For rural areas, agricultural land can be classified into four categories on the basis of the combination of agricultural land type and vulnerability to climate change: (1) multifunctional use (environmental–ecological conservation), (2) maintenance of agricultural production, (3) agricultural–environmental balance, and (4) value-added agricultural production. For each category, adaptation objectives for agricultural land under climate change can be set, providing a basis for adaptation strategies and action plans.

6. Intensive urban development disrupts the balance among environmental, ecological, health, and socioeconomic factors and impedes temperature regulation. Urban areas are typically hotter than suburbs, creating an urban heat island effect. For example, in Taiwan's Taipei and New Taipei City, the basin topography and urban development mean that the temperatures downtown is 3°C higher than that in the suburbs, worsening outdoor thermal conditions.

7. The IPCC AR6 WGIII report (Pathak et al., 2022) notes that energy costs can be reduced through urban and architectural design, which can enhance indoor thermal comfort and promote health. Moreover, by implementing urban greening, river planning, and urban water resource management measures such as permeable pavements and water retention systems, heat accumulation in cities can be mitigated, improving overall thermal comfort.

8. The urban heat island phenomenon in Taiwan is pronounced. As global warming has progressed, the Physiologically Equivalent Temperature (PET) has increased yearly (Figure 4-12). The worsening outdoor thermal conditions in cities render adaptation to the effects of urban heat islands a pressing concern.

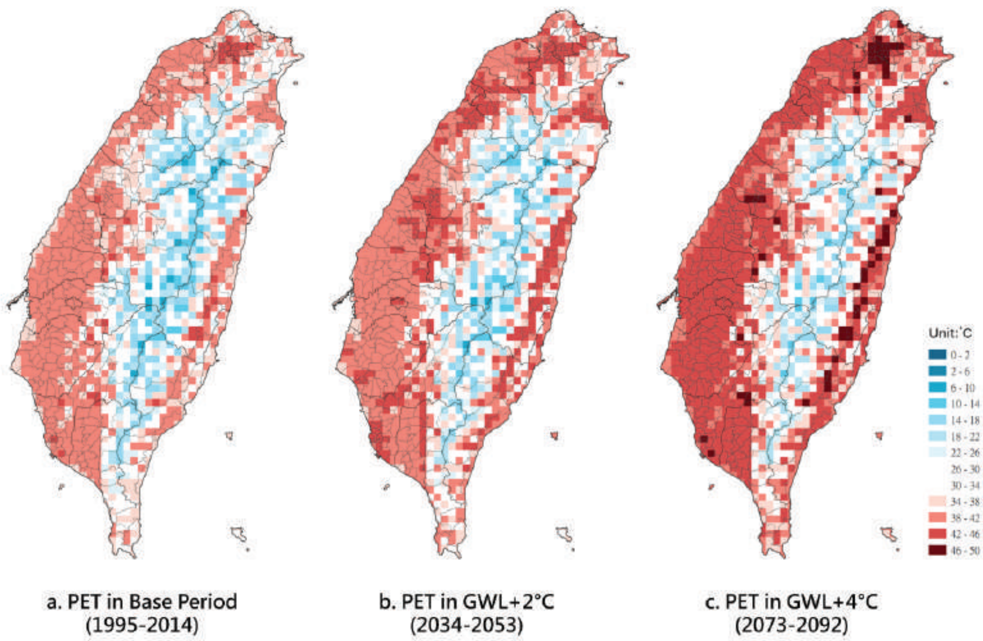

Figure 4-12

PET Distribution Map for Taiwan (Average of July 14:00)

Note: In Figure 4-12 a, b, and c indicate the average PET at 2 pm on the month of July for Taiwan using the climate change projection data for the baseline period and the RCP8.5 global warming scenarios GWL 2°C and GWL 4°C. The figure reveals that the temperature in highly developed downtown areas is substantially higher than that in suburban areas. The pronounced urban heat island phenomenon in Taiwan has resulted in a yearly upward trend in the PET.

9. Although Taiwan's National Land Plan establishes climate assessments and risk case studies for the coastal areas, long-term climate change effects must be considered to address coastal erosion and storm surge flooding. Future research should examine site-specific hazards and make proactive adaptations to reduce these risks.

10. The climate adaptation strategies for individual function zone of National Land Plan are established in the past period. Nevertheless, administrative districts contain multiple space types and require a comprehensive planning approach to address their climate adaptation needs. Integrating climate change into the National Spatial Plan would enable the coordination of adaptation strategies across spaces within administrative areas.

11. This Report recommends focusing future land-use research on the development of comprehensive methodologies of multi-risks assessment by combining land-use change with vulnerability indicators to promote integration of activity system, land uses, and adaptation strategies. This can help facilitate the pre-assessment of the effectiveness of specific adaptation strategies, in terms of the analysis on the initial strategies and future scenarios, including transformational strategies.

12. Urban and rural land includes urban, rural, conservation and coastal space. The measures required to tackle climate change vary across these spatial categories. This Report compiles the results of research on climate change adaptation by spaces of various types. The challenges and advantages of these adaptation strategies are presented, and the impacts of climate change, vulnerabilities, and adaptation strategies are examined (Figure 4-13).

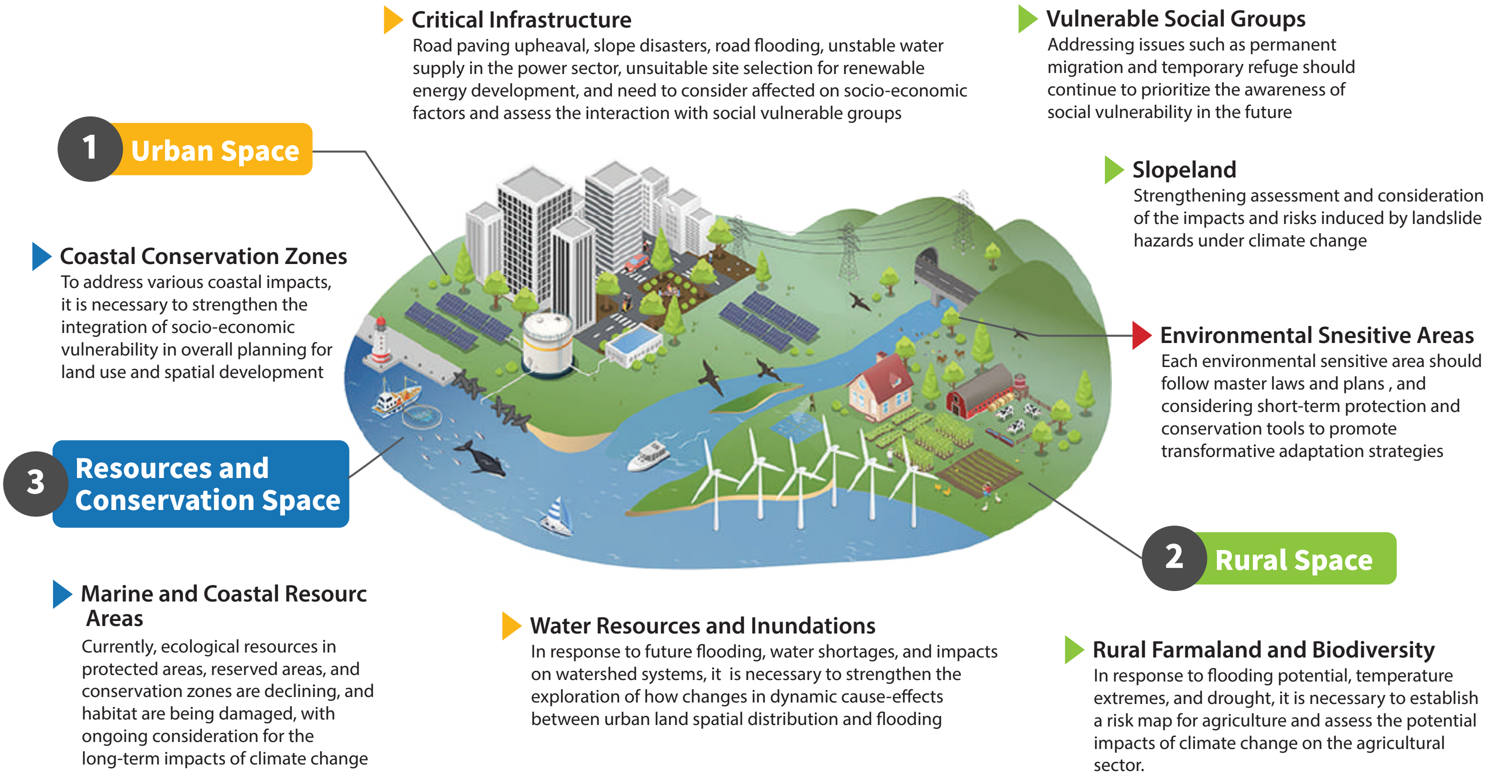

Figure 4-13 Climate Change Impacts on Urban and Rural Spaces

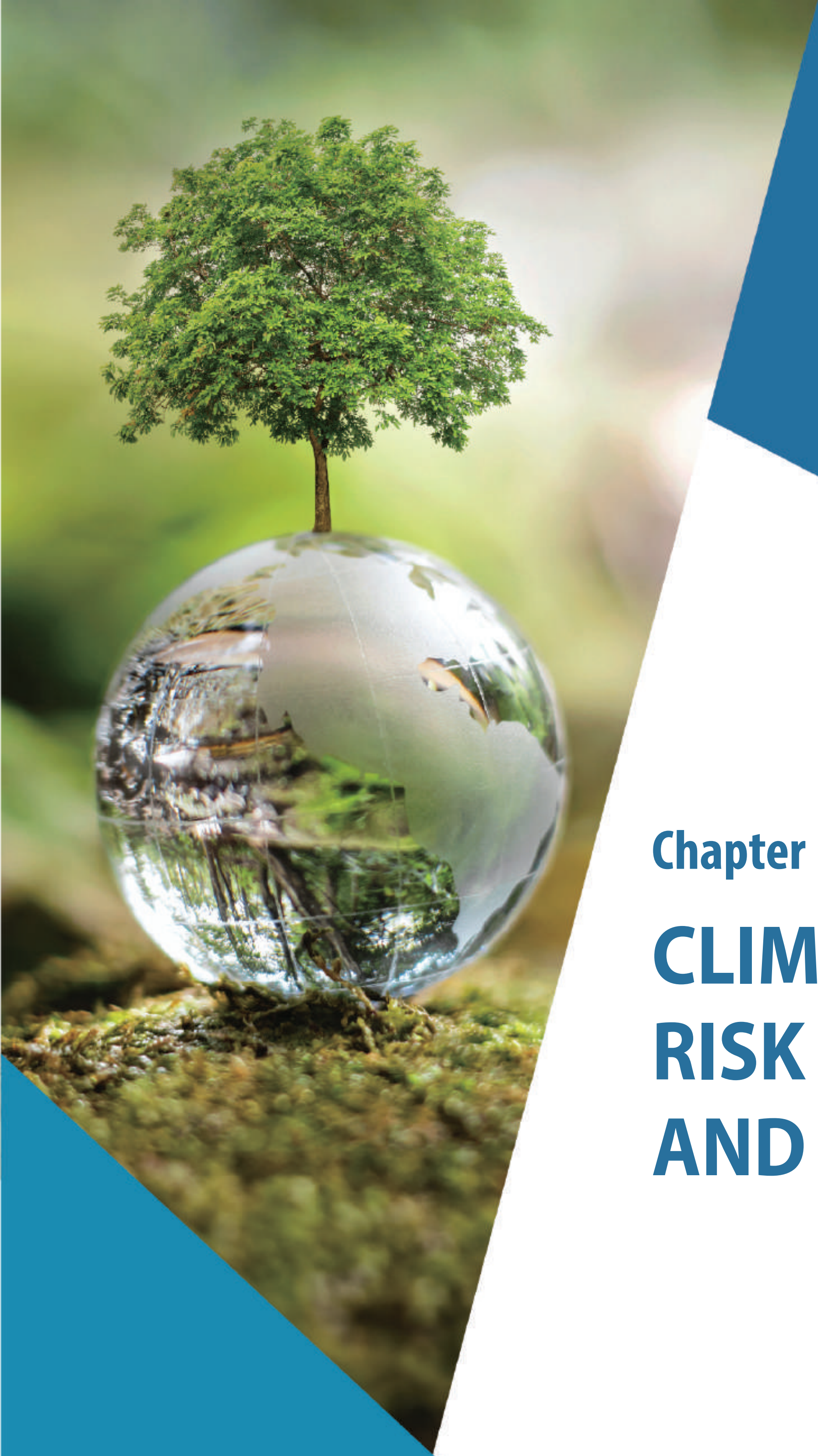

Chapter 5

CLIMATE CHANGE RISK ASSESSMENT AND ADAPTATION

1. This chapter addresses gaps in local data, technologies, tools, and methods for assessing the effects of climate change outlined in Chapter 4 and provides recommendations for improving risk assessment capabilities, such as promoting basic monitoring, developing spatial-scale data, and constructing projective models.

2. This chapter presents suggestions of future research topics such as multi-risks, maladaptation, incremental and transformational adaptation, dynamic adaptation pathways, and adaptation governance across disciplines and sectors.

3. Multi-risks assessment should identify both consequences of short-term disasters and impacts of climate change to assist long-term adaptation planning considering interactions between future land use changes and climate change.

4. Research frameworks for assessing maladaptation comprise (1) pathways framework, (2) precautionary framework, (3) assessment framework, (4) feedback framework, (5) maladaptive evaluation pathways framework with integrated spatial risk analysis, and (6) monitoring and evaluation frameworks for planning national adaptation policies.

5. Incremental adaptation cannot manage climate risks within acceptable levels for increasing impact of climate change, thus transformational adaptation is recommended. This chapter outlines barriers to adopt transformational adaptation in institutions and behaviors, suggesting to incorporate benefits of incremental adaptation into the planning of transformational adaptation for different targeted adaptation time periods Demonstrations of how to undertake these changes with successful transformation adaptation may help overcome social and institutional barriers to successful adaptation.

6. Adaptation planning must consider the extent of climate change and development objectives. The adaptation pathway tool helps governments prioritize risks, assess resources, and determine acceptable risks over specified time frames. Planning diverse adaptation options over time enables communication and the development of consensus among decision-makers and stakeholders.

7. Adaptation and mitigation are conventionally considered and executed as separate actions. Integrating mitigation strategies into adaptation planning can help increase additional benefits and bring non-market benefits while managing the occurrence of maladaptation. Additional recommendations should focus on methods and empirical cases of evaluating cross-policy effectiveness in terms of co-benefits, trade-offs, and synergies.

8. To help administrative departments overcome barriers in adaptation planning and implementation, this chapter addresses social and institutional changes in light of Taiwan's "Climate Change Response Act." Discussions cover mechanisms of governance, barriers to adaptation, groups that are vulnerable to climate change, and regulatory competition.

9. The TCCIP outlines the components of climate change adaptation at each operational stage. Specifically, the framework involves Stage 1, "Identification of Climate Risks and Gaps in Adaptation capacity," and Stage 2, "Adaptation Planning and Implementation." This framework can assist various sectors in developing climate change risk assessments and adaptation plans (Figure 5-1).

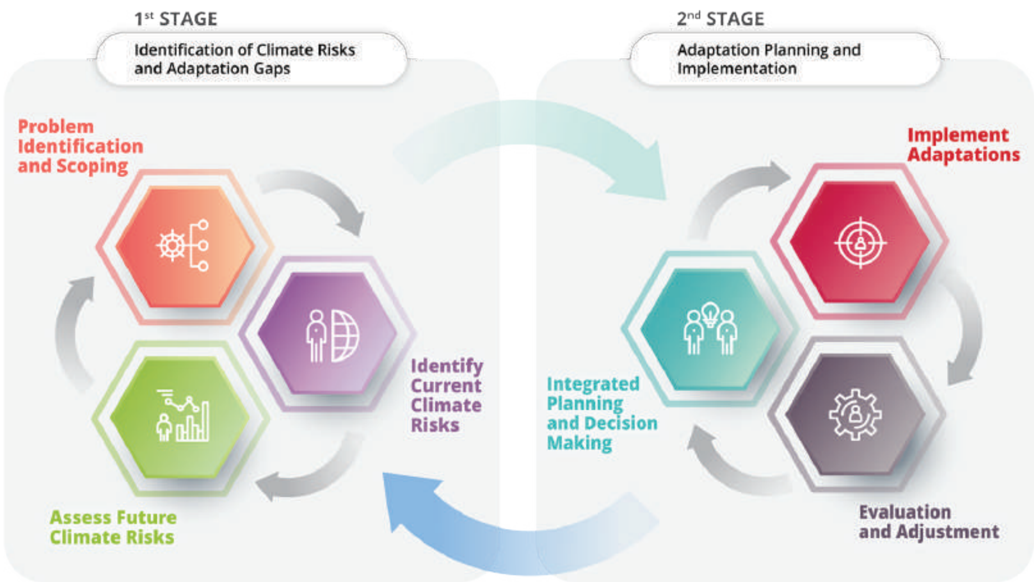

Figure 5-1
The Framework for Climate Change Adaptation Planning

Reference

Alahmad B, Khraishah H, Royé D, Vicedo-Cabrera AM, Guo Y, Papatheodorou SI, Achilleos S, Acquaotta F, Armstrong B, Bell ML, Pan SC, de Sousa Zanotti Stagliorio Coelho M, Colistro V, Dang TN, Van Dung D, De' Donato FK, Entezari A, Guo YL, Hashizume M, Honda Y, Indermitte E, Íñiguez C, … Koutrakis P. (2023). Associations Between Extreme Temperatures and Cardiovascular Cause-Specific Mortality: Results From 27 Countries. Circulation, 147 (1), 35-46. https://doi.org/10.1161/circulationaha.122.061832

Burke, M., González, F., Baylis, P., Heft-Neal, S., Baysan, C., Basu, S., & Hsiang, S. (2018). Higher temperatures increase suicide rates in the United States and Mexico. Nature Climate Change, 8(8), 723-729. https://doi.org/10.1038/s41558-018-0222-x

Chan, S., Shih, W., Chang, A., Shen, S., & Chen, I. (2019). Contrasting forms of competition set elevational range limits of species. Ecology Letters, 22 (10), 1668-1679. https://doi.org/10.1111/ele.13342

Chen, N., Lin, P., & Guo, Y. L. (2019). Long-term exposure to high temperature associated with the incidence of major depressive disorder. Science of The Total Environment, 659, 1016-1020. https://doi.org/10.1016/j.scitotenv.2018.12.434

Chen C. A., Lee M. Y., Liu T. M., Hsu H. H., Lo T. T., Chen Y. M., Tung Y. S., Wu C. Y., Hung H. J., Cheng C. T. & Lin S. Y. (2023) Record-breaking Drought 2020-2021 and Future Projection of Drought Events in Taiwan, Taiwan Climate Change Analysis Series Report 2023. https://tccip.ncdr.nat.gov.tw/km_publish.aspx

Chen, Y., Lin, H., Liou, J., Cheng, C., & Chen, Y. (2022). Assessment of flood risk map under climate change RCP8.5 scenarios in Taiwan. Water, 14 (2), 207. https://doi.org/10.3390/w14020207

Chen, Y.J., Lin, H.J., Liou, J.J., Tung, Y.S. and Chen, Y.M., (2024). Development and application of climate change risk map for landslides. National Science and Technology Center for Disaster Reduction Technical Report, NCDR 112-T10. (in Chinese with English abstract)

Chen, N., Chen, Y., Wu, C., Chen, M., & Guo, Y. (2022). The impact of heavy precipitation and its impact modifiers on shigellosis occurrence during typhoon season in Taiwan: A casecrossover design. Science of The Total Environment, 848, 157520. https://doi.org/10.1016/j.scitotenv.2022.157520

Cheng, C. T., Chien Y. T., Lin S. Y., Wang C. Y. (2024). Differences in future projections of typhoons near Taiwan in different climate periods. National Science and Technology Center for Disaster Reduction Technical Report NCDR 112-T24. (in Chinese with English abstract)

Chung, Y., Lim, Y., Honda, Y., Guo, Y. L., Hashizume, M., Bell, M. L., Chen, B., & Kim, H. (2015). Mortality related to extreme temperature for 15 cities in Northeast Asia. Epidemiology, 26 (2), 255-262. https://doi.org/10.1097/ede.0000000000000229

Hintsala, H., Kenttä, T. V., Tulppo, M., Kiviniemi, A., Huikuri, H. V., Mäntysaari, M., KeinänenKiukaannemi, S., Bloigu, R., Herzig, K., Antikainen, R., Rintamäki, H., Jaakkola, J. J., & Ikäheimo, T. M. (2014). Cardiac Repolarization and autonomic regulation during short-term cold exposure in hypertensive men: An experimental study. PLoS ONE, 9 (7), e99973. https://doi.org/10.1371/journal.pone.0099973

Hsieh, S., Hsieh, C., Tseng, C., & Yiin, L. (2020). Allergic rhinitis: Association with air pollution and weather changes, and comparison with that of allergic conjunctivitis in Taiwan. Atmosphere, 11(11), 1152. https://doi.org/10.3390/atmos11111152

IPCC, 2021: Technical Summary. InClimate Change 2021: The Physical Science Basis. Contribution of Working Group I to the Sixth Assessment Report of the Intergovernmental Panel on Climate Change [Masson-Delmotte, V., P. Zhai, A. Pirani, S.L. Connors, C. Péan, S. Berger, N. Caud, Y. Chen, L. Goldfarb, M.I. Gomis, M. Huang, K. Leitzell, E. Lonnoy, J.B.R. Matthews, T.K. Maycock, T. Waterfield, O. Yelekçi, R. Yu, and B. Zhou (eds.)]. Cambridge University Press, Cambridge, United Kingdom and New York, NY, USA, (pp.33-144). https://doi.org/10.1017/9781009157896.002.

Kim, Y., Kim, H., Gasparrini, A., Armstrong, B., Honda, Y., Chung, Y., Ng, C. F., Tobias, A., Íñiguez, C., Lavigne, E., Sera, F., Vicedo-Cabrera, A. M., Ragettli, M. S., Scovronick, N., Acquaotta, F., Chen, B., Guo, Y. L., Seposo, X., Dang, T. N., … Hashizume, M. (2019). Suicide and ambient temperature: A multi-country multi-city study. Environmental Health Perspectives, 127 (11). https://doi.org/10.1289/ehp4898

Kim, J., Shin, J., Lim, Y., Honda, Y., Hashizume, M., Guo, Y. L., Kan, H., Yi, S., & Kim, H. (2016). Comprehensive approach to understand the association between diurnal temperature range and mortality in East Asia.Science of The Total Environment, 539, 313-321. https://doi.org/10.1016/j.scitotenv.2015.08.134

Lan, W. H., Kuo, C. Y., Kao, H. C., Lin, L. C., Shum, C. K., Tseng, K. H., & Chang, J. C. (2017).Impact of geophysical and datum corrections on absolute sea-level trends from tidegauges around Taiwan, 1993–2015.Water, 9 (7), 480.

Lee, H., Wu, Y., Kusumaning Asri, A., Chen, T., Pan, W., Yu, C., Su, H., & Wu, C. (2020). Linkage between residential green spaces and allergic rhinitis among Asian children (case study: Taiwan). Landscape and Urban Planning, 202, 103868. https://doi.org/10.1016/j.landurbplan.2020.103868

Lee, M., Huang, W., Shen, Y., Weng, J., Semedi, B., Wang, Y., & Chan, J. (2021). Long-term observations of Interannual and decadal variation of sea surface temperature in the Taiwan Strait. Journal of Marine Science and Technology, 29 (4). https://doi.org/10.51400/2709-6998.1587

Lee, M. A., S. Mondal, J. H. Wu & M. Boas, (2022). Total Catch Variability in the Coastal Waters of Taiwan in relation to Climatic Oscillations and possible impacts. Journal of the Fisheries Society of Taiwan, 49, 127-143. https://doi.org/10.29822/JFST.202206_49(2).0006

Li, C., Chytrý, M., Zelený, D., Chen, M., Chen, T., Chiou, C., Hsia, Y., Liu, H., Yang, S., Yeh, C., Wang, J., Yu, C., Lai, Y., Chao, W., & Hsieh, C. (2013). Classification of Taiwan forest vegetation. Applied Vegetation Science, 16(4), 698-719. https://doi.org/10.1111/avsc.12025

Lin, W., Lin, Y., Lien, W., Wang, Y., Lin, C., Chiou, C., Anthony, J., & Crossman, N. (2014). Expansion of protected areas under climate change: An example of mountainous tree species in Taiwan. Forests, 5(11), 2882-2904. https://doi.org/10.3390/f5112882

Lin, H.-Y, (2020). Predicting the potential distributions of plant species and forests in Taiwan under present and future climates. Doctoral dissertation. National Taiwan University, Taipei, Taiwan.

Lu, M., & Huang, J. (2023). Predicting negative effects of climate change on Taiwan' s endemic bumblebee Bombus formosellus. Journal of Insect Conservation, 27 (1), 193-203. https://doi.org/10.1007/s10841-022-00415-1

Lung, S.C.C., Chou, S.W., Chen, J.P., Wen, P.C., Su, H.J.J., Tsai, I.C., and Chen, Y.S. (2018). Science Plan of Climate Change and Health Adaptation. Journal of Taiwan Land Research, 21(2), 209-239.

McCormack, M. C., Belli, A. J., Waugh, D., Matsui, E. C., Peng, R. D., Williams, D. L., Paulin, L., Saha, A., Aloe, C. M., Diette, G. B., Breysse, P. N., & Hansel, N. N. (2016). Respiratory effects of indoor heat and the interaction with air pollution in chronic obstructive pulmonary disease. Annals of the American Thoracic Society, 13(12), 2125-2131. https://doi.org/10.1513/annalsats.201605-329oc

McRae, C. J., Keshavmurthy, S., Meng, P., Rosset, S. L., Huang, W., Chen, C. A., Fan, T., & Côté, I. M. (2022). Variable responses to chronic and acute elevated temperature of three coral species from reefs with distinct thermal regimes. Marine Biology, 169 (7). https://doi.org/10.1007/s00227-022-04071-6

Mora, C., McKenzie, T., Gaw, I. M., Dean, J. M., Von Hammerstein, H., Knudson, T. A., Setter, R. O., Smith, C. Z., Webster, K. M., Patz, J. A., & Franklin, E. C. (2022). Over half of known human pathogenic diseases can be aggravated by climate change. Nature Climate Change, 12(9), 869-875. https://doi.org/10.1038/s41558-022-01426-1

Pathak, M., Slade, R., Shukla, P.R., Skea, J., Pichs-Madruga, R., & Ürge-Vorsatz, D. (2022). Technical Summary. In: Climate Change 2022: Mitigation of Climate Change. Contribution of Working Group III to the Sixth Assessment Report of the Intergovernmental Panel on Climate Change [P.R. Shukla, J. Skea, R. Slade, A. Al Khourdajie, R. van Diemen, D. McCollum, M. Pathak, S. Some, P. Vyas, R. Fradera, M. Belkacemi, A. Hasija, G. Lisboa, S. Luz, J. Malley, (eds.)]. Cambridge University Press, Cambridge, UK and New York, NY, USA. https://doi.org/10.1017/9781009157926.002

Peng, S., Huang, J., Sheehy, J. E., Laza, R. C., Visperas, R. M., Zhong, X., Centeno, G. S., Khush, G.S., & Cassman, K. G. (2004). Rice yields decline with higher night temperature from global warming. Proceedings of the National Academy of Sciences, 101 (27), 9971-9975. https://doi.org/10.1073/pnas.0403720101

Suk, J. E., Vaughan, E. C., Cook, R. G., & Semenza, J. C. (2020). Natural disasters and infectious disease in Europe: A literature review to identify cascading risk pathways. European Journal of Public Health, 30(5), 928-935. https://doi.org/10.1093/eurpub/ckz111

Tran, H. M., Chen, T., Lu, Y., Tsai, F., Chen, K., Ho, S., Wu, C., Wu, S., Lee, Y., Chung, K. F., Kuo, H., Lee, K., & Chuang, H. (2022). Climate-mediated air pollution associated with COPD severity. Science of The Total Environment, 843, 156969. https://doi.org/10.1016/j.scitotenv.2022.156969

Tsai, I. C., Hsieh, P. R., Hsu, H. H., Tung, Y. S., Chen, Y. M., & Cheng, C. T. (2024). Climate change induced impacts on PM2.5 in Taiwan under 2 and 4° C global warming. Atmospheric Pollution Research, 15 (6) 102106. https://doi.org/10.1016/j.apr.2024.102106

Tittensor, D. P., Novaglio, C., Harrison, C. S., Heneghan, R. F., Barrier, N., Bianchi, D., Bopp, L., Bryndum-Buchholz, A., Britten, G. L., Büchner, M., Cheung, W. W., Christensen, V., Coll, M., Dunne, J. P., Eddy, T. D., Everett, J. D., Fernandes-Salvador, J. A., Fulton, E. A., Galbraith, E. D., … Blanchard, J. L. (2021). Next-generation ensemble projections reveal higher climate risks for marine ecosystems. Nature Climate Change, 11 (11), 973-981. https://doi.org/10.1038/s41558-021-01173-9

Wang, Y., & Wu, C. (2019). Enhanced warming and intensification of the Kuroshio extension, 1999–2013. Remote Sensing, 11 (1), 101. https://doi.org/10.3390/rs11010101

Water Resources Planning Branch of the Water Resources Agency, Ministry of Economic Affairs (2022) Impact Assessment of Climate Change on Water Resources of Major River Basins.

Watson, J. T., Gayer, M., & Connolly, M. A. (2007). Epidemics after natural disasters. Emerging Infectious Diseases, 13(1), 1-5. https://doi.org/10.3201/eid1301.060779

Witt, C., Schubert, J. A., Jehn, M., Holzgreve, A., Liebers, U., Endlicher, W., & Scherer, D. (2015). The effects of climate change on patients with chronic lung disease. Deutsches Ärzteblatt international. https://doi.org/10.3238/arztebl.2015.0878

Yamanaka, G., Nakano, H., Sakamoto, K., Toyoda, T., Urakawa, L. S., Nishikawa, S., Wakamatsu, T.,Tsujino, H., & Ishikawa, Y. (2021). Projected climate change in the western North Pacific at the end of the 21st century from ensemble simulations with a high-resolution regional ocean model.Journal of Oceanography, 77 (3), 539-560. https://doi.org/10.1007/s10872-021-00593-7

Zhong, J., Lee, Y., Hsieh, C., Tseng, C., & Yiin, L. (2019). Association between the first occurrence of allergic conjunctivitis, air pollution and weather changes in Taiwan. Atmospheric Environment, 212, 90-95. https://doi.org/10.1016/j.atmosenv.2019.05.045